The Journal of Neuroscience, January 15, 1997, 17(2):676–696

# Temporal and Spatial Expression Patterns of Transgenes Containing Increasing Amounts of the *Drosophila* Clock Gene *period* and a *lacZ* Reporter: Mapping Elements of the PER Protein Involved in Circadian Cycling

**Ralf Stanewsky,[1] Brigitte Frisch,[1] Christian Brandes,[1] Melanie J. Hamblen-Coyle,[1] Michael Rosbash,[1,2] and Jeffrey C. Hall[1]**

[1]*Department of Biology and* [2]*Howard Hughes Medical Institute, Brandeis University, Waltham, Massachusetts 02254*

*This article is dedicated to Brigitte Frisch. She found delight in her work and life. She believed that everyone had something important to offer and made us all feel special. Her humor and strength will always be remembered.*

Rhythmic oscillations of the PER protein, the product of the *Drosophila period* (*per*) gene, in brain neurons of the adult fly are strongly involved in the control of circadian rhythms. We analyzed temporal and spatial expression patterns of three *per–reporter* fusion genes, which share the same 4 kb regulatory upstream region but contain increasing amounts of *per*'s coding region fused in frame to the bacterial *lacZ* gene. The fusion proteins contained either the N-terminal half (SG), the N-terminal two-thirds (BG), or nearly all (XLG) of the PER protein. All constructs led to reporter signals only in the known *per*-expressing cell types within the anterior CNS and PNS. Whereas the staining intensity of SG flies was constantly high at different Zeitgeber times, the *in situ* signals in BG and XLG flies cycled with ~24 hr periodicity in the PER-expressing brain cells in wild-type and $per^{01}$ loss of function flies. Despite the rhythmic fusion-gene expression within the relevant neurons of $per^{01}$ BG flies, their locomotor activity in light/dark cycling conditions and in constant darkness was identical to that of $per^{01}$ controls, uncoupling protein cycling from rhythmic behavior. The XLG construct restored weak behavioral rhythmicity to (otherwise) $per^{01}$ flies, indicating that the C-terminal third of PER (missing in BG) is necessary to fulfill the biological function of this clock protein.

*Key words: circadian rhythms;* period *gene;* lacZ *reporter; Lateral Neurons; fusion proteins; locomotor behavior; immunochemistry*

The *period* (*per*) gene is thought to be a central component of the circadian clock in *Drosophila*. Mutations in this gene abolish ($per^{01}$), shorten ($per^{S}$, $per^{Clk}$, and $per^{T}$), or lengthen ($per^{L}$) daily locomotor activity rhythms that persist in constant darkness (DD) in wild-type flies (Konopka and Benzer, 1971; Dushay et al., 1992; Konopka et al., 1994). Under normal light/dark (LD) conditions, $per^{S}$ and $per^{L}$ mutants show phase advances or delays of their evening activity peaks, whereas $per^{01}$ mutants do not entrain at all and simply react to the LD changes (Hamblen-Coyle et al., 1992; Wheeler et al., 1993) (see Fig. 12).

*per* RNA and PER protein fluctuate in abundance with 24 hr periods (Hardin et al., 1990; Zerr et al., 1990; Zeng et al., 1994). Expression of the *per* gene in $per^{01}$, $per^{S}$, and $per^{L}$ is affected in the same manner as locomotor behavior, indicating a molecular feedback loop in which the PER protein regulates its own transcription (for review, see Hall, 1995; Rosbash, 1995). Mutations in a different clock gene, *timeless* (*tim*) also produce arrhythmic ($tim^{01}$) and period-altered ($tim^{SL}$) behavior (Sehgal et al., 1994; Rutila et al., 1996). The products of the *tim* gene undergo similar fluctuations as those of *per*, and both PER and TIM proteins can dimerize *in vivo* (Sehgal et al., 1995; Zeng et al., 1996). $tim^{01}$ or $per^{01}$ mutations result in loss of rhythmic RNA expression of the other (nonmutated) gene, indicating that both genes are necessary for establishing the molecular feedback loop in which the PER–TIM heterodimer is thought to play an important role (Zeng et al., 1996).

Behavioral analysis of genetic mosaics expressing PER in certain lateral brain neurons (LNs) of $per^{01}$ flies is sufficient to restore rhythmic behavior under DD conditions, suggesting that these cells have pacemaker function (Ewer et al., 1992). Analysis of PER coding transgenes showing rhythmic expression in the LNs of $per^{01}$ flies was consistent with these results: the transgenics were able to entrain to LD cycles and showed rhythmic behavior under DD conditions (Frisch et al., 1994; Vosshall and Young, 1995).

A genomic 4.2 kb DNA fragment upstream of *per*'s coding region was shown to drive rhythmic RNA expression of reporter genes fused to this sequence when endogenous PER protein is present in these flies (Hardin et al., 1992). Fusion of *per*-regulatory sequences directly to *lacZ* did not lead to cycling of β-galactosidase (β-GAL) levels in a $per^{+}$ genetic background, whereas this 5′-flanking DNA from the *per* locus and half of its coding region were reported to permit β-GAL to fluctuate with a 24 hr period (Zwiebel et al., 1991). That result did not prove reproducible, which was one of the reasons that prompted our

Received July 8, 1996; revised Oct. 31, 1996; accepted Nov. 5, 1996.

This work was supported by National Institutes of Health Grant GM-33205 to J.H. and a postdoctoral fellowship from the Deutsche Forschungsgemeinschaft to R.S. We thank Maki Kaneko and Creston Jamison for assistance with the scoring of staining intensities and for comments on this manuscript, Jill Lefferson for helping to produce germline transformants, Neal White for behavioral analysis, and Ed Dougherty for photographic assistance.

Correspondence should be addressed to Dr. Jeffrey C. Hall, Department of Biology, 235 Bassine Building, Brandeis University, 415 South Street, Waltham, MA 02254-9110.

Dr. Brandes' current address: Biozentrum der Universität Wien, 1030 Wien, Austria.

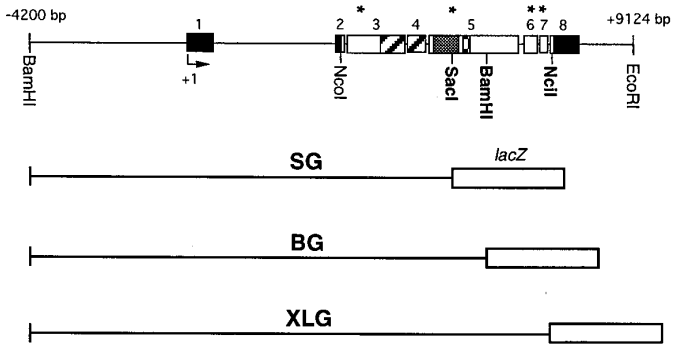


*Figure 1.* Structure of *per–lacZ* fusion genes analyzed for temporal and spatial expression. In the *top panel*, the structure of a 13.2 kb genomic DNA fragment containing the *per* gene is shown. This construct restores rhythmic behavior after transformation into $per^{01}$ mutants (Citri et al., 1987). The *solid line* represents upstream untranscribed regulatory sequences as well as introns and 3′ untranscribed DNA. The *bars* reflect exon sequences; *solid parts* designate untranslated and *open bars* protein-coding DNA sequences. *Striped portions* represent the PAS domain, which can function as an intermolecular protein dimerization motive (residues 240–496) (Burbach et al., 1992). *Shaded areas* represent the C domain involved in intramolecular protein interactions (residues 524–685, Huang et al., 1995), and *checked areas* represent the GT repeats, which vary in number among different *Drosophila melanogaster* strains (e.g., 20 Gly-Thr pairs in the wild-type strain *Oregon-R*) (Yu et al., 1987). Potential PEST sequences, identified by the program PESTFIND (Rechsteiner et al., 1987) are indicated by *asterisks* and extend from residues 135 to 162 (exon 3), 652 to 664 (exon 5), 1184 to 1215 (exon 6), and 1242 to 1256 (also showing the highest PEST score, exon 7). The *arrow* indicates *per*'s transcription start site (*+1*). Translation starts at the *Nco*I site and stops 32 bp 3′ of the *Nci*I site. The different *per–lacZ* fusion genes contain various amounts of this genomic *per* DNA fragment, fused in frame to the *E. coli lacZ* gene. They all share the same 5′ regulatory region (from the *Bam*HI site at −4200) and transcribed sequences up to the *Sac*I site in exon 5 (including the PAS domain), where the SG fragment is fused to *lacZ.* SG contains only one complete PEST sequence and is missing parts of the C domain and all of the GT repeat. The BG construct contains additional *per*-coding DNA up to the *Bam*HI site in exon 5, including two PEST sequences as well as the complete C domain and GT repeat. XLG extends to the *Nci*I site in exon 8, including two additional PESTs that are missing in BG. Note that this construct does not quite encode the full-length PER protein (see Materials and Methods).

analysis of a series of *per–lacZ* fusion constructs, each sharing the same 5′ regulatory sequences but with increasing amounts of *per*'s coding region (Fig. 1). Thus, we mapped regions of the *per* gene product that are necessary to allow PER-like protein turnover. To ask whether the cycling of a certain fusion protein could be independent of endogenous PER, we also analyzed the temporal expression of these transgenes in a $per^{01}$ background. Analysis of locomotor behavior was performed under LD and DD conditions to determine which fusion proteins might mediate rhythmic behavior.

## MATERIALS AND METHODS

### *Generation of* per–lacZ *fusion constructs*

The structure and generation of the SG construct has been described previously (Liu et al., 1988). It contains a 4.2 kb 5′-flanking region that is part of a 13.2 kb genomic *per* fragment; the latter almost completely rescues the effects of the arrhythmic $per^{01}$ mutation (Citri et al., 1987; Yu et al., 1987; Dushay et al., 1992). In addition to this upstream region, SG contains *per* DNA coding for ~50% (638 amino acids) of the N-terminal PER protein (up to the *Sac*I site, therefore called *S*G) (Fig. 1) fused in frame to the bacterial *lacZ* gene.

The generation of the BG construct is described elsewhere (Dembinska et al., 1997). It contains the same 4.2 kb 5′-flanking region as SG and encodes 868 amino acids of PER, corresponding to the N-terminal two-thirds of this protein (up to the *Bam*H1 site and therefore called BG) (Fig. 1) fused in frame to the *lacZ* gene (as above).

The XLG construct was generated as follows. First, the CaspeR *lacZ* transformation vector (Thummel et al., 1988) was modified by replacing the *Bam*HI and *Pst*I restrictions sites with *Xho*I and *Not*I sites after Klenow treatment and blunt-end ligation of the respective linkers. The *Xho*I site was created to allow in-frame cloning of genomic *per* DNA to *lacZ*. A 6.4 kb genomic *per* DNA fragment containing sequences from −4200 bp to +2267 bp (the bp numbers are with reference to the transcription start of the *per* gene) was cut with *Not*I and *Xba*I and ligated into the *Not*I and *Xba*I sites of the transformation vector (the *Xba*I site is located between the *Xho*I and *Not*I sites of the modified vector). In a different step, a clone containing genomic *per* DNA from the *Xba*I site at +2267 to a *Xho*I site at position +6658 was generated [the *Xho*I site was generated after first filling in the original NciI site at position +6658 with Klenow and then blunt-ligating it to a filled in *Xho*I site of pBluescript II KS(+)]. To create the final construct, this 4.4 kb *Xba*I/*Xho*I fragment was ligated in frame into the *Xba*I/*Xho*I sites of the transformation vector. This construct contains DNA coding for nearly the whole PER protein, except 10 amino acids at the C-terminal end, normally encoded by DNA extending from the *Nci*I site at position +6658 to the translational stop codon TAG at position +6690. Because the *Nci*I site was replaced by *Xho*I and a *Xho*I linker was used to create this restriction site in the *lacZ* gene, this construct was named *XL*G.

### *Stocks and P-element transformation*

The genetic variants used for this study are described in Lindsley and Zimm (1992). Flies were raised on a cornmeal, sugar, yeast, and Tegosept medium (the latter being a mold inhibitor) on a 12:12 hr LD cycle (lights on at 8 A.M.)

Two independently isolated SG lines, carrying this *per–lacZ* fusion gene inserted into the *X* (SG10) or the second chromosome (SG3) (Liu et al., 1988; Zwiebel et al., 1991) were used in this study. Both lines were obtained after transforming $per^{01}$;$ry^{506}$ embryos. To generate a $per^{+}$ SG10 strain, the $per^{01}$ SG10 chromosome was recombined with a $per^{+}$ $w$ $sn^{3}$ chromosome to replace the loss-of-function mutation with *per*'s normal allele (Ewer et al., 1992).

One transgenic BG line was obtained after transforming $per^{01}$;$ry^{506}$ embryos with the BG construct (X. Liu, personal communication). In this line, the P-element is inserted on the third chromosome and causes lethality when flies are homozygous for the insertion; this line is balanced with the multiply inverted third chromosome *In(3LR)TM2, ry Ubx* and was therefore named BG/*TM2* (indicating that flies from this stock carry only one copy of the BG construct). The BG transposon in BG/*TM2* was mobilized by crossing that strain to a transposase-producing Δ2-3 strain (Robertson et al., 1988); this resulted in the homozygous-viable BG6 strain, in which the transgene is located on the second chromosome.

The XLG-A and XLG-B strains were generated after transforming *Df(1)w* embryos with the XLG construct (carrying the mini-$white^{+}$ gene as selectable marker). Transformations were performed using standard techniques (Rubin and Spradling, 1982); transposase was supplied by co-injection of the helper plasmid pUChsπΔ2-3 (Laski et al., 1986). Two transformed lines were recovered, derived from different injected embryos. The locations of the insertions were determined genetically by crossing transformant flies to second and third chromosomal balancer chromosomes. The XLG-A and XLG-B lines carry their (homozygous-viable) insertions on the second chromosome. To analyze these transgenes in a $per^{01}$ background, the *Df(1)w* chromosome (which carries $per^{+}$) was replaced by an *X* chromosome carrying $per^{01}$ $w$ $sn^{3}$.

### *Histochemistry*

Transgenic males carrying either the SG-, BG-, or XLG-*lacZ* fusion genes were exposed to at least three 12:12 hr LD cycles at 25°C before sectioning. For the cycling experiments, flies were collected at two different Zeitgeber times (ZTs) in the case of SG and XLG (ZT12 and ZT24 for SG, ZT9 and ZT21 for XLG; ZT24 defines "lights on" and ZT12 "lights off") and at four different times in the case of BG (ZT3, ZT9, ZT15, and ZT21). For the time points at which the flies had to be collected in the dark, vials were moved (in darkness) from the incubator to a small light-tight container where they were kept until they were either anesthetized or embedded in a tissue-freezing medium (TBS).

*Immunohistochemistry.* Flies were anesthetized, their wings and legs removed, and the specimens transferred to an Eppendorf tube containing 1 ml ice-cold fixing solution (4% paraformaldehyde in 0.1 M sodium phosphate buffer, pH 7.0). After fixing them for 4 hr at 4°C on a rotating

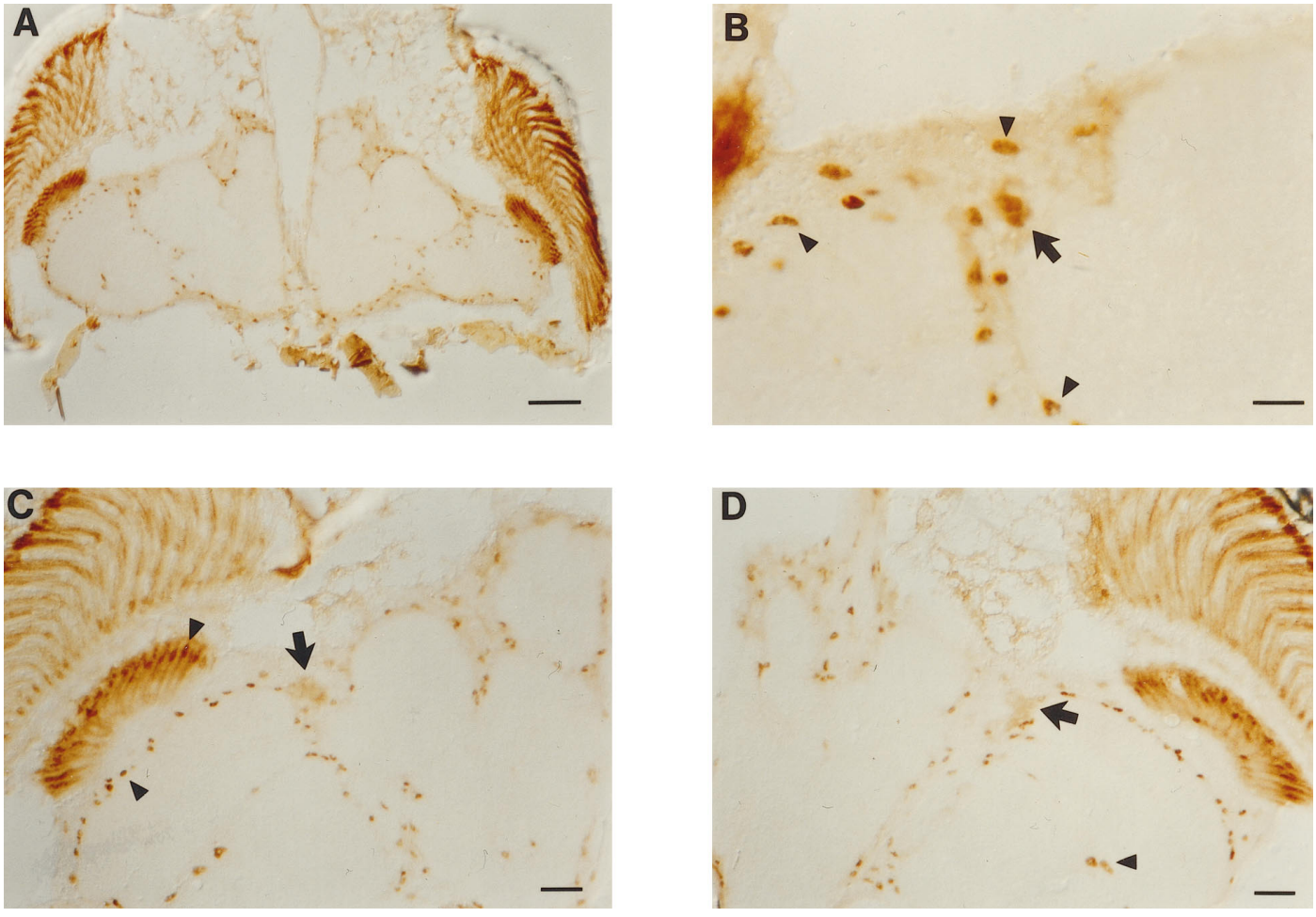


*Figure 2.* Distribution of anti-β-GAL immunoreactivity in a $per^{+}$ SG3 transgenic adult male. *A*, Staining pattern at the level of the esophagus, in a horizontal section (the others depicted here are in the same plane). Scale bar, 40 μm. *B*, Magnification of *A*; *arrow* points to a group of the $LN_v$ (relatively ventral LNs; see Ewer at al., 1992); *arrowheads* point to glia cells in the outer rim of the medulla, in the cortex, and to glia located at the border between the cortex and the neuropil of the central brain. Scale bar, 8 μm. *C*, A different section located just ventral to that in *A* and *B*; the *arrow* points to $LN_v$, *arrowheads* to glia cells located in the lamina and the outer rim of the medulla. Scale bar, 12.5 μm. *D*, A section showing not only $LN_v$ (*arrow*), but also glia cells in the second optic chiasm (*arrowhead*). Scale bar, 12.5 μm.

mixer, the fixing solution was removed and the flies were washed four times for 10 min in 0.1 M phosphate buffer, pH 7.4, at 4°C. After the last wash, flies were incubated overnight in 25% sucrose in 0.1 M phosphate buffer, pH 7.4, at 4°C. Flies were frozen in tissue-freezing medium, and horizontal sections (10 μm) of individual specimens were made on a cryostat microtome (SLEE). Sections were then transferred to glass slides, dried for 1 hr, and rinsed in 0.1 M phosphate buffer, pH 7.4, for 10 min and in PBS two times for 10 min each at room temperature. Each slide was preincubated for 1 hr at room temperature with 400 μl PBS containing 3% normal horse serum (NHS), 0.1% Triton X-100, and 0.1% BSA. Sections were then incubated overnight at 4°C with a monoclonal mouse anti-β-GAL antibody (Promega, Madison, WI) diluted 1:2000 in PBS containing 3% NHS, 0.03% Triton X-100, and 0.1% BSA. On the next day, slides were rinsed three times for 10 min each at room temperature (as for all the following washes and incubations) in PBS containing 0.03% Triton X-100 and 0.1% BSA and then incubated for 1 hr with a 1:200 dilution (see above) of a secondary biotinylated horse anti-mouse antibody (Vector Laboratories, Burlingame, CA). After rinsing the sections three times for 10 min each in PBS containing 0.03% Triton X-100 and 0.1% PBS, then two times for 10 min each in the same solution without Triton X-100, the Vectastain ABC ELITE Kit (Vector) was used to amplify the staining signal. Slides were washed again two times for 10 min each in PBS containing 0.1% BSA and three times for 10 min each in PBS before they were developed with DAB, as described in Siwicki et al. (1988) with minor modifications. All sections included in the cycling analysis were incubated with 0.3 mg/ml DAB solution for exactly 3 min. Slides were then baked with Crystal Mount (Biomeda), and coverslips were mounted with DPX (Fluka, Ronkonkoma, NY). Sections were viewed and photographed using Nomarski optics and a Zeiss Axiophot light microscope.

Anti-PER stainings were performed by incubating fly sections (see above) with a polyclonal rabbit anti-PER antibody, which was raised against full-length PER protein expressed in a baculovirus expression system (Liu et al., 1992). Anti-PER antibodies were used in a final concentration of 1:6000 after preabsorbing the serum against $per^{01}$ embryos. Signals were visualized after incubation with a secondary biotinylated donkey anti-rabbit antibody (1:200) and DAB, as described above.

*X-gal staining.* Stainings with 5-bromo-4-cloro-3-indolyl-β-D-galactopyranoside (X-gal) were carried out on 10 μm frozen horizontal sections, as described in Liu et al. (1988), except that slides were mounted and photographed as described above (for the antibody stainings).

*Scoring of staining intensities.* In the case of the BG construct, transgenic males from the BG/*TM2* strain in a $per^{+}$ and $per^{01}$ background were collected at four different time points during a 24 hr cycle (see above). Five males ($per^{+}$ genetic background) or six males ($per^{01}$ background) per time point were analyzed. After staining and mounting, the slides were coded and scored by three different investigators, who inspected the sections at 160× magnification under the microscope. Levels of staining were subjectively scored using an intensity scale of 1 to 4, in increments of 0.5 (1 = no detectable staining above background, 4 = most intense staining). Scoring was carried out separately for the following three *per*-expressing tissues in the head: photoreceptor (PR) cells, glia, and

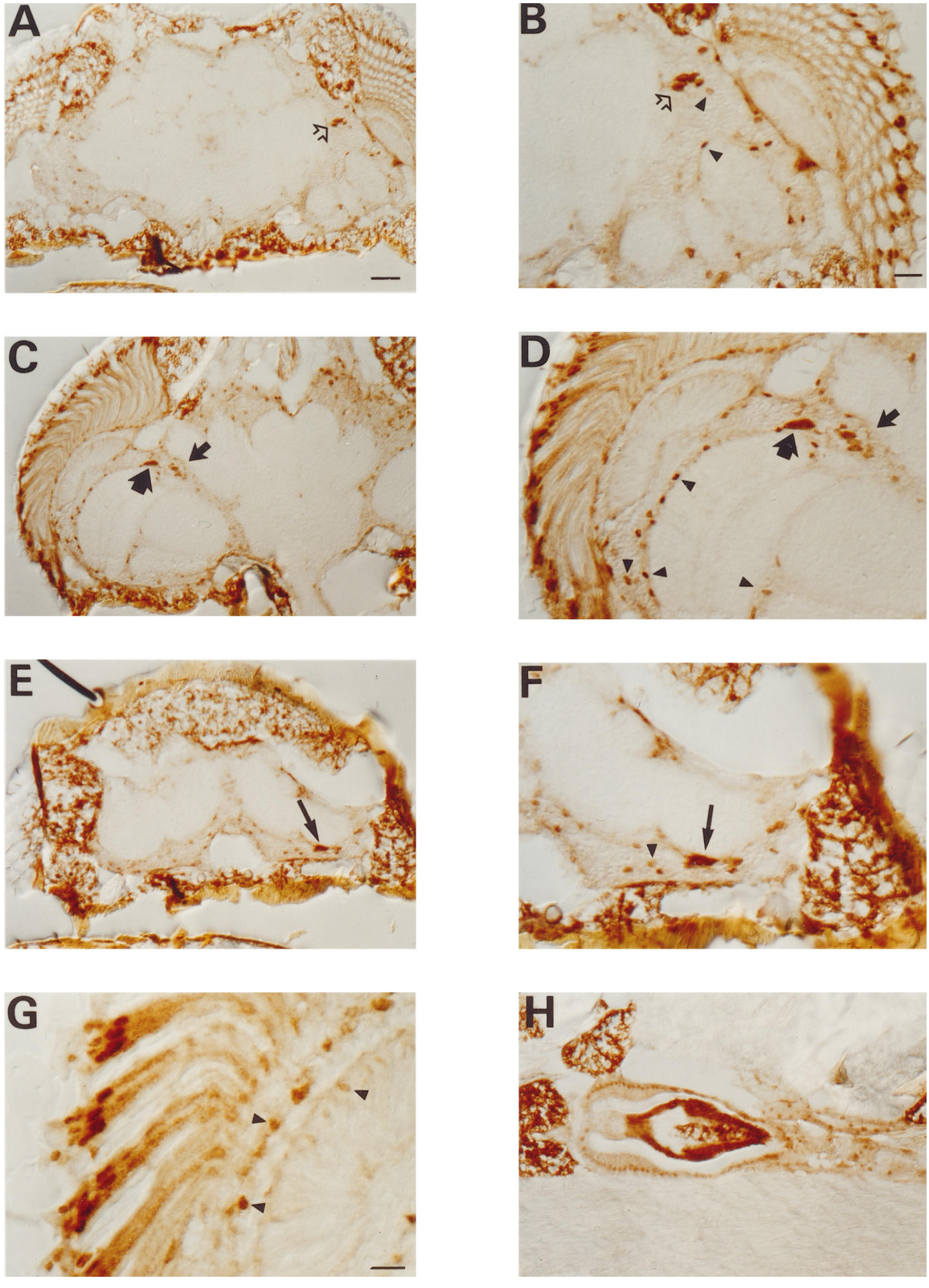


*Figure 3.* Pattern of *per*-expressing cells in a $per^{+}$ BG transgenic adult at ZT21. This male carried the BG construct heterozygous with a balancer chromosome (*TM2*; see Materials and Methods) and was stained with anti-β-GAL antibody. *A*, The *open arrow* points to $LN_d$ (relatively dorsal LNs; see Ewer et al., 1992). Scale bar, 25 μm *B*, High-magnification view of *A*; four to five $LN_d$ (diameter, ~6 μm) lie close together; *arrowheads* point to glia in the cortex, adjacent to the neurons, and to glia bordering the medulla. Scale bar, 12.5 μm. *C*, A large oval cell of the $LN_v$ group (*large arrow*); the *smaller arrow* points to four neurons of smaller diameter (~6 μm). *D*, Higher magnification of *C*; *arrowheads* point to glial cells at the outer rim of the medulla and to glia in the second optic chiasm. *E*, DNs. *F*, Higher magnification of *E*, showing two overlapping DNs present in this section (diameter, ~8 μm); the *arrowhead* indicates cortical glia. *G*, PR staining (*left* part of the image); the *arrowheads* point to glia in the lamina and in the layer between the PRs and lamina. Scale bar, 8 μm. *H*, Staining in the cardia. Magnifications in *C*, *E*, and *H* as in *A*; in *D* and *F* as in *B*.

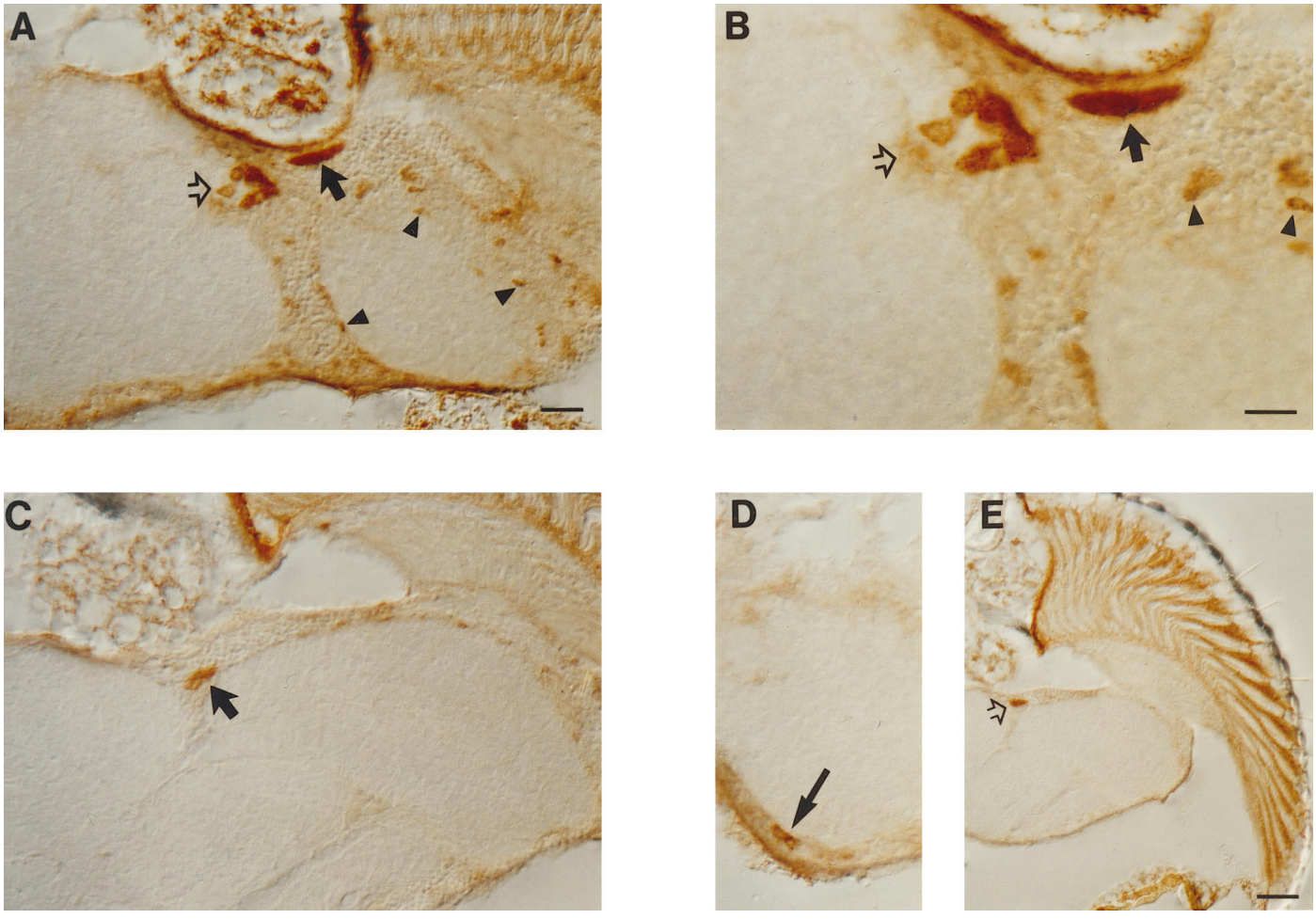


*Figure 4.* *per*-Expressing cells in the head of a $per^{+}$ XLG-B transgenic adult at ZT21. The sections of the male were stained with anti-β-GAL antibody (staining of this line is more intense than in XLG-A, but the spatial pattern is identical; compare Fig. 10) (also data not shown). *A*, Six $LN_d$ cells (*open arrow*) are visible in this section (diameter, ~5–6 μm); the *solid arrow* points to two large cells (diameter, ~11 μm) from the relatively dorsal region of the $LN_v$ group; *arrowheads* indicate glia cells bordering the medulla. Scale bar, 12.5 μm. *B*, Higher magnification of *A*. Scale bar, 8 μm. *C*, The *solid arrow* points to $LN_v$; four cells of smaller size (diameter, ~4–5 μm) are visible in this plane. *D*, DNs (*arrow*); note that the nucleus seems stained lighter than the surrounding cytoplasm (diameter, ~3–5 μm). Magnifications in *C* and *D* are as in *A*. *E*, PR staining, which appears mainly cytoplasmic (the nuclei cannot be distinguished from the soma); the *open arrow* points to a group of $LN_d$. Scale bar, 25 μm.

*per*-expressing LNs (cf. Zerr et al., 1990). Final (to be plotted) scores were calculated as follows. First, the mean for each animal was determined as the average of the value given by each of the three investigators, then the five or six means for all animals sectioned at the same time were averaged to calculate the final mean (± SEM) for a given genotype, tissue, and time (see Results; see Fig. 8). In the case of the SG construct type, males from the two transgenic lines SG3 and SG10 [the former in a $per^{+}$ ($n$ = 10) and a $per^{01}$ ($n$ = 8) background, the latter in a $per^{+}$ background only ($n$ = 10)] were sectioned at two opposite ZTs (see above) and stained with X-gal. Collections were made from incubators that were kept on opposite phases [LD and dark/light (DL)] so that pairs of flies with the same genotype but entrained to opposite ZTs could be collected and processed at the same time (each pair was processed on a given experimental day). To standardize the scoring of the staining intensity, photographs (all at the same exposure) of each fly brain, at the level of the esophagus, were taken. These images of fly brains, from flies sectioned on the same day, were then ranked by three different observers (each fly was given one rank, representing an average staining intensity of PRs, glia, and the ventral group of *per*-expressing LNs). These photographs were then decoded, and ranks given to a pair of flies, with the same genotype and opposite ZT, were compared. If the fly at ZT12 was given a higher rank (e.g., stronger staining intensity) compared with its partner at ZT24, the pair was classified as "higher staining at ZT12"; and vice versa. If both flies of a pair turned out to have the same rank, they were classified as "equal" (see Fig. 6).

### *Immunoblotting*

Flies from the XLG-A and XLG-B transgene strains, in a $per^{+}$ and a $per^{01}$ background, were entrained for at least 3 d in 12:12 hr LD cycles, as described for the histochemistry experiments. Animals from all four genotypes were collected and immediately frozen on dry ice at six different ZTs (ZT2, ZT6, ZT10, ZT14, ZT18, and ZT22). Total fly-head protein extracts were prepared from 100 to 200 heads of each collection, as described in Edery et al. (1994). Equal amounts of each extract (~100 μg) were mixed with 5× SDS sample buffer (Laemmli, 1970) and separated on 5.7% polyacrylamide (29.6:0.4, acrylamide:bisacrylamide ratio)/SDS gels. After electrophoresis, proteins were electroblotted to nitrocellulose membranes (12–14 hr with 150 mA in a buffer containing 20% methanol, 0.1% SDS, 14.2 mM Tris, 192 mM Glycin). To ensure that the transfer of the 300 kd XLG fusion proteins had been complete, gels were stained with Coomassie brilliant blue. The quality of protein transfer and the (intended) equal loading were checked by staining the proteins on the nitrocellulose membrane, using the reversible Ponceau S stain (Sigma, St. Louis, MO). After blocking with 1% BSA in a solution containing 140 mM NaCl, 10 mM Tris/HCl, ph 7.5, 0.05% Tween 20 (TBST) membranes were incubated with a polyclonal rabbit anti-PER (see above) or a mouse monoclonal anti-β-GAL (Promega) antibody (both 1:10,000 diluted in 5% nonfat dry milk in TBST) for 2 hr. Filters were washed one time for 15 min and three times for 5 min in TBST and incubated for 30 min with a secondary HRP-coupled anti-rabbit or anti-mouse antibody (Amer-

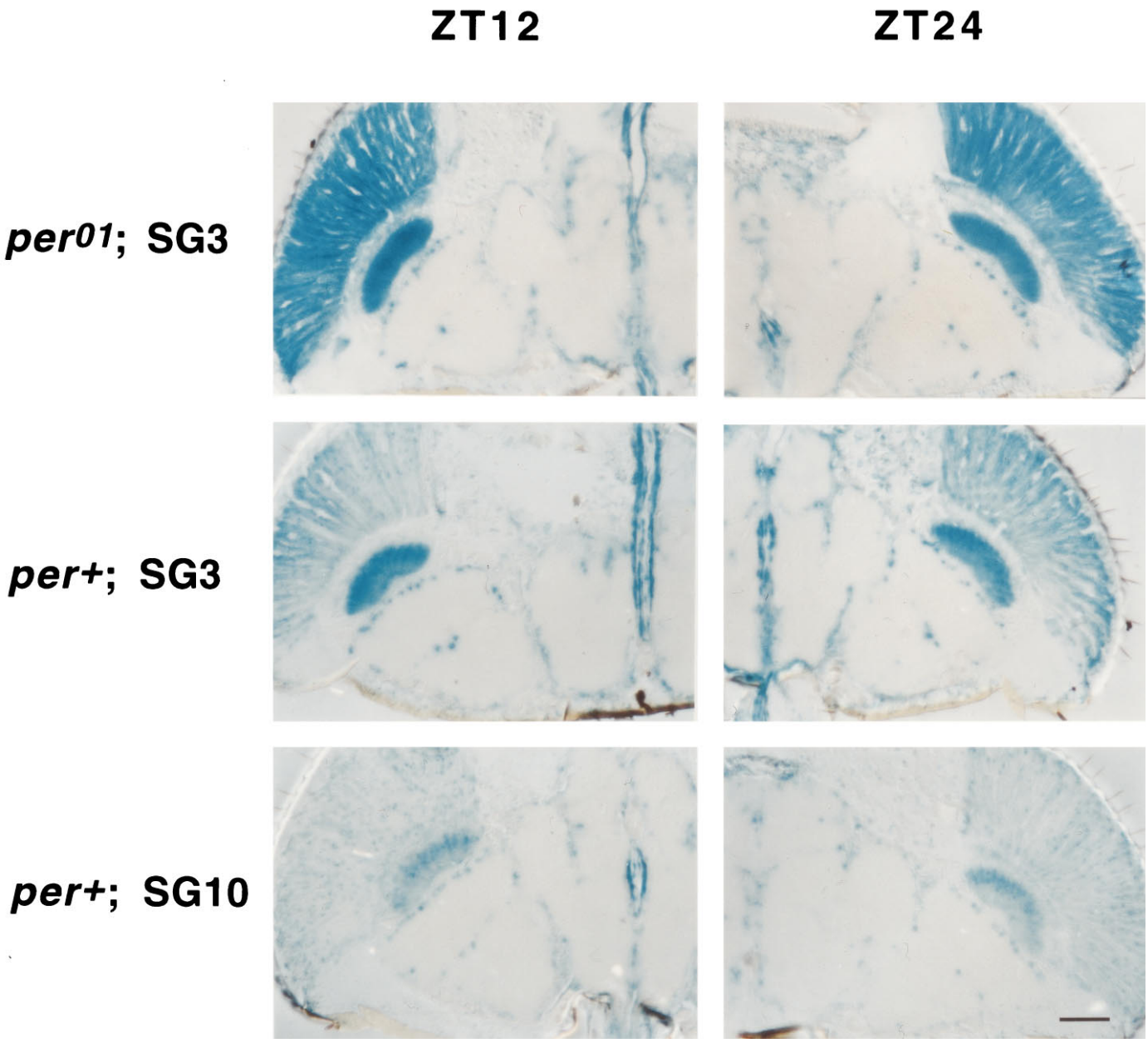


*Figure 5.* Temporal expression in heads of SG transgenic flies. Pairs of males carrying the same *per* allele were sectioned and stained with X-gal at opposite ZTs. In contrast to PER, which is highly abundant late at night (ZT24) and nearly undetectable by the end of the day (ZT12), the SG fusion protein shows no such fluctuations (compare ZT12 with ZT24). The reporter activity was at a constantly high level in PR cells, glia, and LNs in $per^{+}$ and $per^{01}$ genetic backgrounds, for both the SG3 and SG10 transgenic flies (data not shown for $per^{01}$ SG10). The same results were obtained after staining SG transgenics with anti-β-GAL antibody (data not shown).

sham, Arlington Heights, IL), respectively. After washing (see above), proteins were visualized using the Enhanced Chemi-Luminescence Kit (Amersham) followed by autoradiography. Typically, exposures were for 1–60 sec. Band intensities were quantified after exposing membranes to chemiluminescence sensitive screens (usually 10 times longer than for x-ray exposures) and by subsequent imaging of exposed screens in a phosphoimager (Bio-Rad, Hercules, CA). After staining a membrane with the anti-PER antibody, the same membrane was stripped (in 100 mM β-mercaptoethanol, 2% SDS, 62.5 mM Tris/HCl, pH 6.7, for 30 min at 50°C), blocked, and incubated with anti-β-GAL antibody, as described above. Amplitudes of protein cycling were calculated after first setting the highest expression values (as obtained from the phosphoimager data) in each experiment equal to 1, followed by dividing the mean of the two highest values (usually ZT18 and ZT22) by that of the two lowest values (usually ZT2 and ZT6).

### *Circadian behavioral rhythms*

Locomotor activity of adult males was monitored automatically, as described in Hamblen et al. (1986). Data were processed and analyzed, as described in Hamblen-Coyle et al. (1992).

Flies were kept under 12:12 hr LD conditions at 25°C for 7 or 11 d, depending on the experiment. Recording of the locomotor activity data began after 1 d in LD conditions. On day 8 or 12, respectively, the lights stayed off, such that the flies were subsequently monitored in DD conditions for the next 12–14 d. To determine the period of free-running rhythms, data collected under DD conditions were searched for periodocities using the $\chi^2$ periodogram (Sokolove and Bushell, 1978). Significant periods were determined as described by Hamblen et al. (1986).

To determine the exact position of the morning and evening activity peaks in LD conditions, a program called Phase was applied (for details,

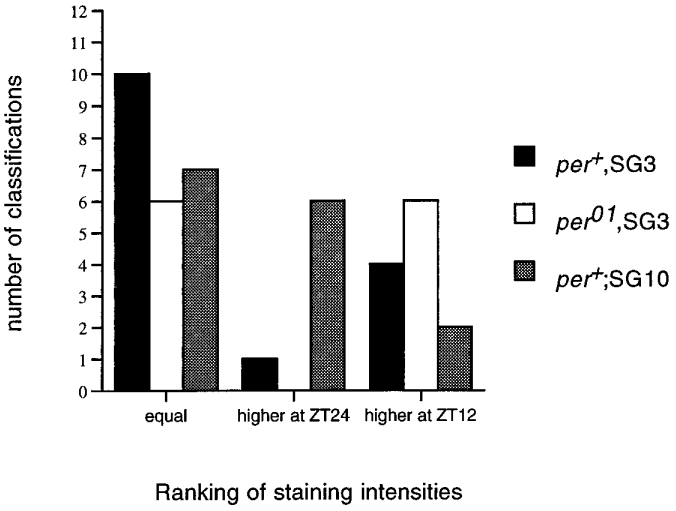


*Figure 6.* Quantification of staining intensities for the SG3 and SG10 *per–lacZ* transformants. Three observers were asked to rank (X-gal-mediated) staining intensities of fly brains sectioned at ZT24 and ZT12 on the same day (see Materials and Methods). The intensity for a given pair of flies (with the same *per* genotype) was classified as "higher at lights on" (ZT24), "higher at lights off" (ZT12), or "equal." For the $per^+$ SG3/SG3 and $per^+$ SG10 transgenics, five pairs of flies were scored, and for $per^{01}$ SG3/SG3, four pairs (resulting in a total of 15 classifications for the $per^+$ genetic background and 12 classifications in the $per^{01}$ background). The majority of fly pairs from all genotypes showed equal staining at both time points or higher staining at lights off (in contrast to wild-type PER or BG- and XLG-*per–lacZ* fusion proteins, which stain most intensely around lights on) (Zerr et al., 1990; present study).

see Hamblen-Coyle et al., 1992). It allows an objective determination of an activity peak (with respect to times of environmental transitions in LD cycles) for each fly on a given day; then a mean (per day) value is computed for an individual for which successive cycles involve the same environmentally cycling conditions. These (per fly) mean phase values were used in a (nonparametric) Mann–Whitney *U* test to perform statistical comparisons among the different genotypes. The software (Hamblen-Coyle et al., 1992) was also used to compute group phase values for all the animals of a given genotype tested (see Table 1).

## RESULTS

### Spatial expression pattern of SG, BG, and XLG transgenes at a high time point

*In situ* expression of the *per* gene has been revealed by using *per–lacZ* fusion genes and by anti-PER antibody stainings (Liu et al., 1988, 1991, 1992; Siwicki et al., 1988; Ewer et al., 1992). In *Drosophila* heads, *per* is expressed in certain neurons, in PRs R1–R8, in the ocelli, and in glia cells of the optic lobes and the central brain. The *per*-expressing neurons consist of two classes, known as Lateral Neurons (LNs), which are located in the cortex between the dorsal anterior brain and the medulla, and dorsal neurons (DNs), located in the posterior dorsal-most cortex. The LNs were reported to consist of two groups: a more dorsally located cluster of approximately three to seven cells on each side of the brain called the *dorsal* LNs ($LN_d$) and another, more ventral cluster of at least eight cells called the *ventral* LNs ($LN_v$). For the DNs, between 2 and 10 cells can be found on each side of the brain (Ewer et al., 1992; Helfrich-Förster and Homberg, 1993; Frisch et al., 1994; Helfrich-Förster, 1995).

To compare the spatial distribution of the three different PER–β-GAL fusion proteins used in this study with that of wild-type PER protein, sections of SG, BG, and XLG transgenic flies were stained by application of anti-β-GAL antibodies (Fig. 1). To allow comparisons of expression levels among the different transgenes, all flies were fixed for sectioning late at night (ZT21), when PER is expressed at its maximum levels (Zerr et al., 1990). In agreement with earlier studies (Liu et al., 1988; Ewer et al., 1992), the SG fusion protein is expressed in all known *per*-expressing cells, although several differences (quantitative and qualitative) were observed. Figure 2 demonstrates head expression of the SG3 transgenic line, which shows the same staining pattern and intensity differences in the various cell types that were reported previously for the SG10 strain (*per–β-gal*) (see Materials and Methods; see also Ewer et al., 1992). Compared with PER expression, SG signals appear to be more intense in glia (in Fig. 2*C*, *arrowheads*) and PRs, whereas staining in the LNs (*arrows*) is much fainter (compare Fig. 2 with Ewer et al., 1992). Also, the number of stained glial cells in the optic lobes and especially in the central brain seems to be larger compared with that of PER positive cells (Fig. 2) (cf. Ewer et al., 1992). In addition the fusion protein is detectable in both nuclei and cytoplasm of LNs and PRs (glial cells are too small to make this distinction), whereas PER is predominantly nuclear late at night (Fig. 2) (cf. Ewer et al., 1992; Liu et al., 1992, Curtin et al., 1995).

The larger BG fusion protein is also expressed in all known *per*-expressing cells; however, in contrast to SG, its expression seems more closely to reflect the wild-type expression pattern (Fig. 3). All types of neurons (DN, $LN_d$, $LN_v$) were stained intensely. This fusion protein fills up the somata, which made it possible to distinguish the different sizes (and shapes) of the neurons. The DNs are a loose cluster of cells. The two neurons shown in Figure 3, *E* and *F*, have a diameter of ~8 μm. The $LN_d$ usually form a tight cluster of ~six cells; their diameter is ~6 μm (Fig. 3*A*,*B*). This group is usually difficult to identify in the SG strains, probably because of the weak SG expression in the LNs in general (see above). The $LN_v$ consist of two different-sized cell types: four large oval neurons (diameter, ~13 μm) and four to six smaller cells (diameter, 6 μm) (Fig. 3*C*,*D*) (cf. Helfrich-Förster and Homberg, 1993; Helfrich-Förster, 1995). In most samples, the locations of the $LN_v$ span 30–40 μm in the dorsal to ventral direction. Usually the large neurons are slightly dorsal to the smaller neurons, but there is variability in the arrangement of these cells.

By focusing through the soma of the LNs, one can usually distinguish the nucleus from cytoplasm by slightly lighter staining in the former compartment (see Fig. 3*B* for the $LN_d$ and *D* for the $LN_v$). Thus, the BG fusion protein can enter the nucleus, but it is clearly not predominantly nuclear as is PER at this time of the LD cycle (Curtin et al., 1995). Glial staining in the BG transgenic type was generally less intense and restricted to fewer cells than glial

→

*Figure 7.* Cycling immunoreactivity of the BG fusion protein. Males carrying this transgene heterozygous with the *TM2* balancer and, expressing either $per^+$ or $per^{01}$, were sectioned and stained with anti-β-GAL antibodies. All sections shown are at the level of the esophagus, where strong staining of the ventral group of LNs ($LN_v$) can be observed at a high time point (compare Fig. 3). $LN_v$ are marked by *arrows*, glia cells by *arrowheads*. The *left* column shows staining in a $per^+$ background at four different ZTs; at ZT3, strong staining of the $LN_v$, glia, and PR cell nuclei can be observed. Scale bar, 20 μm. At ZT9, only weak staining in all three cell types is detectable. Scale bar, 40 μm. At ZT15 staining is still weak in the $LN_v$ and (*Figure legend continues*)

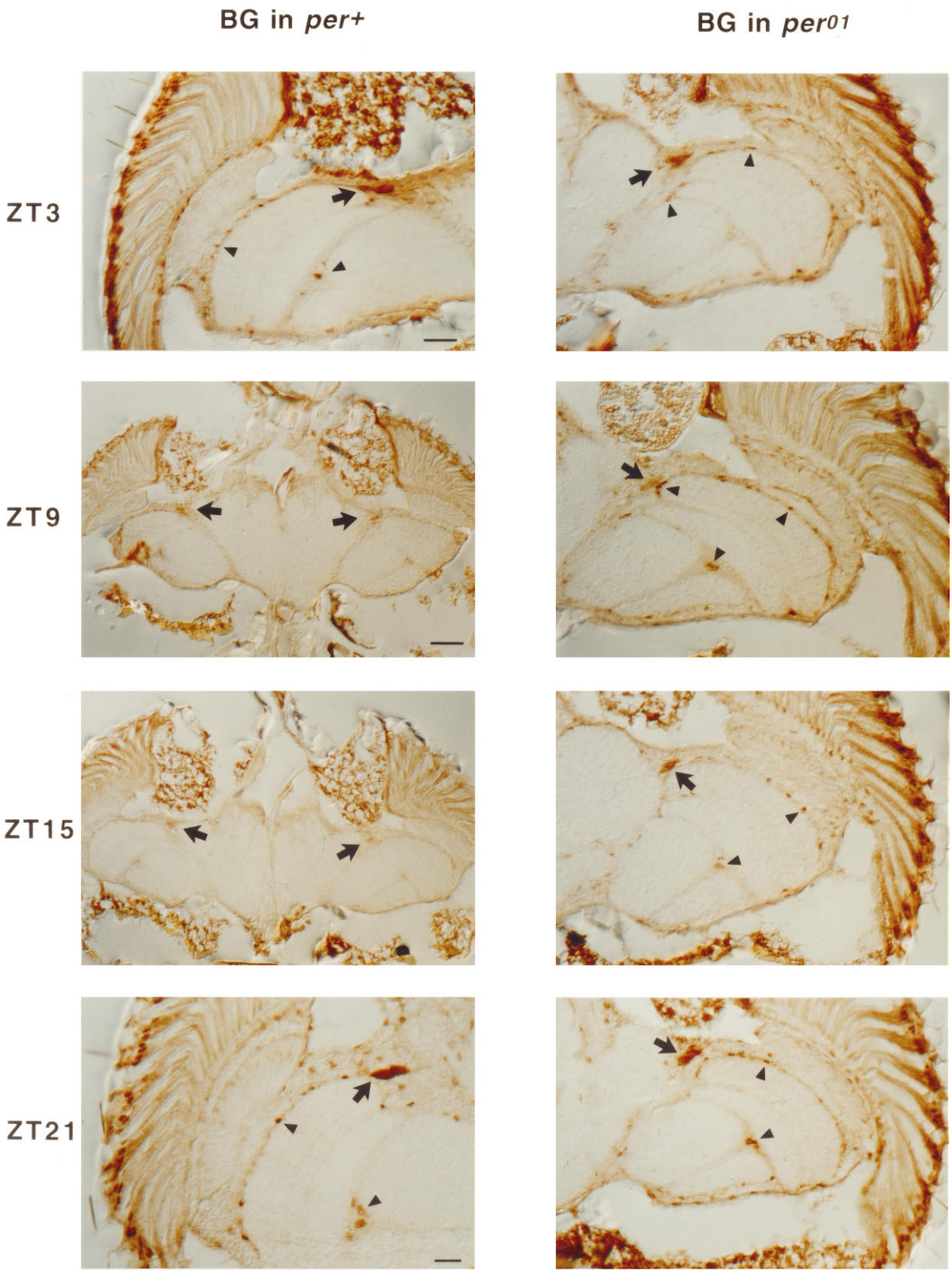


glia cells, although the signal in the cytoplasm of the PRs seems stronger compared with ZT9 (the magnification for both of these time points is the same); staining in all three cell types is again very prominent at ZT21. Scale bar, 12.5 $\mu$m. The temporal pattern in the *per* $^{01}$ background (*right column*) differs from that just described. At ZT3, prominent staining in the $LN_v$, glia, and nuclei of the PRs is visible, in contrast to the *per*$^+$-expressing flies, and the staining intensity in the PRs and glia remains at a high level at ZT9. Only the $LN_v$ show a decrease in signal strength at that time point. At ZT15, the staining became stronger again in the $LN_v$ and remained high in PRs and glia. At ZT21, staining intensities in all three cell types was as high as in the *per*$^+$ background. Magnifications for all *per* $^{01}$ time points are as in *per*$^+$ at ZT3.

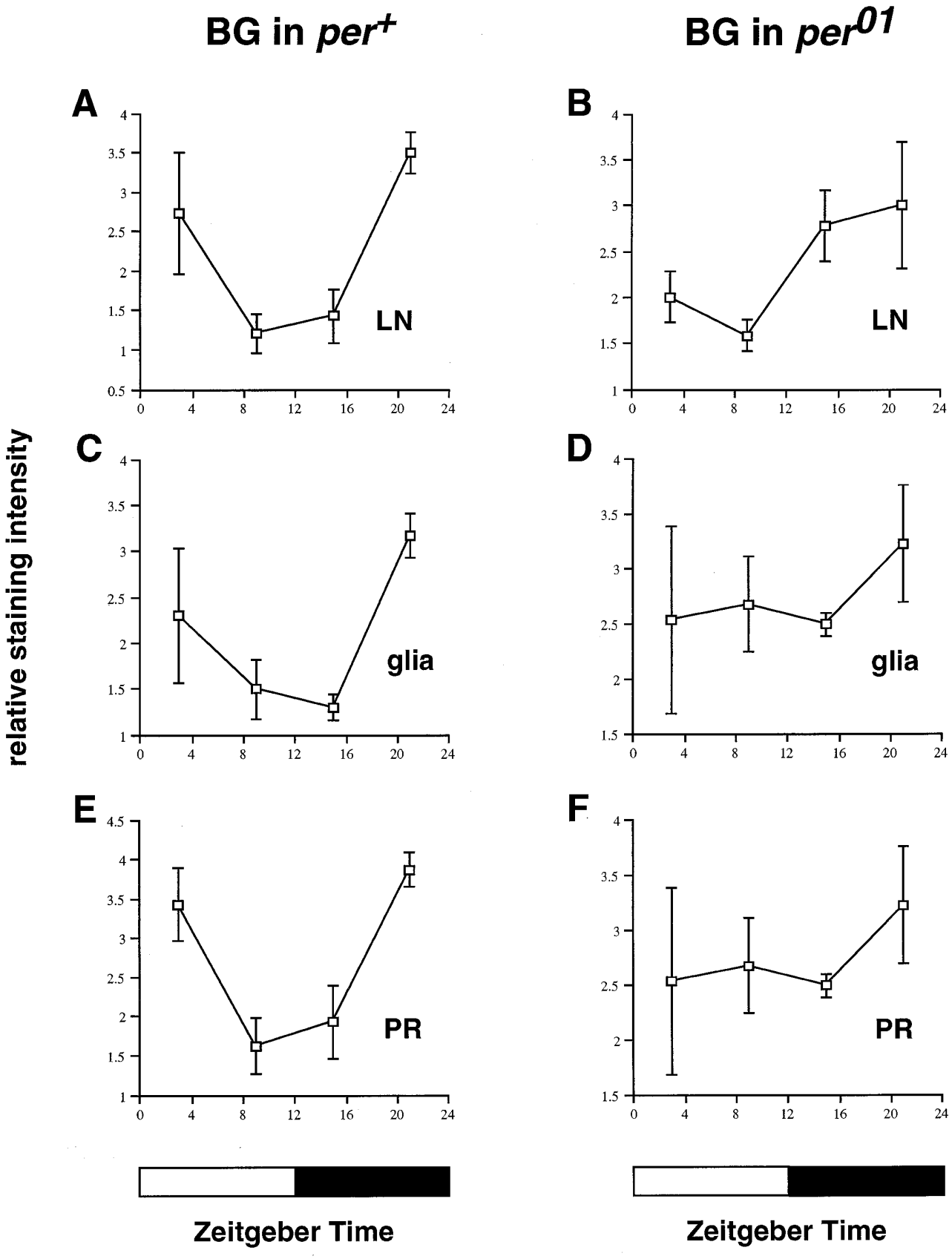


*Figure 8.* Quantification of BG-mediated staining intensities. Sections from $per^{+}$ or $per^{01}$ BG/*TM2* males were stained with anti-β-GAL-antibody. Flies were entrained and collected under 12:12 hr LD conditions. Five ($per^{+}$) or six ($per^{01}$) flies were sectioned and stained at each time point. The staining intensities in the LNs, glia, and PRs of each fly were subjectively scored by three observers (who were unaware of either genotype (*Figure legend continues*)

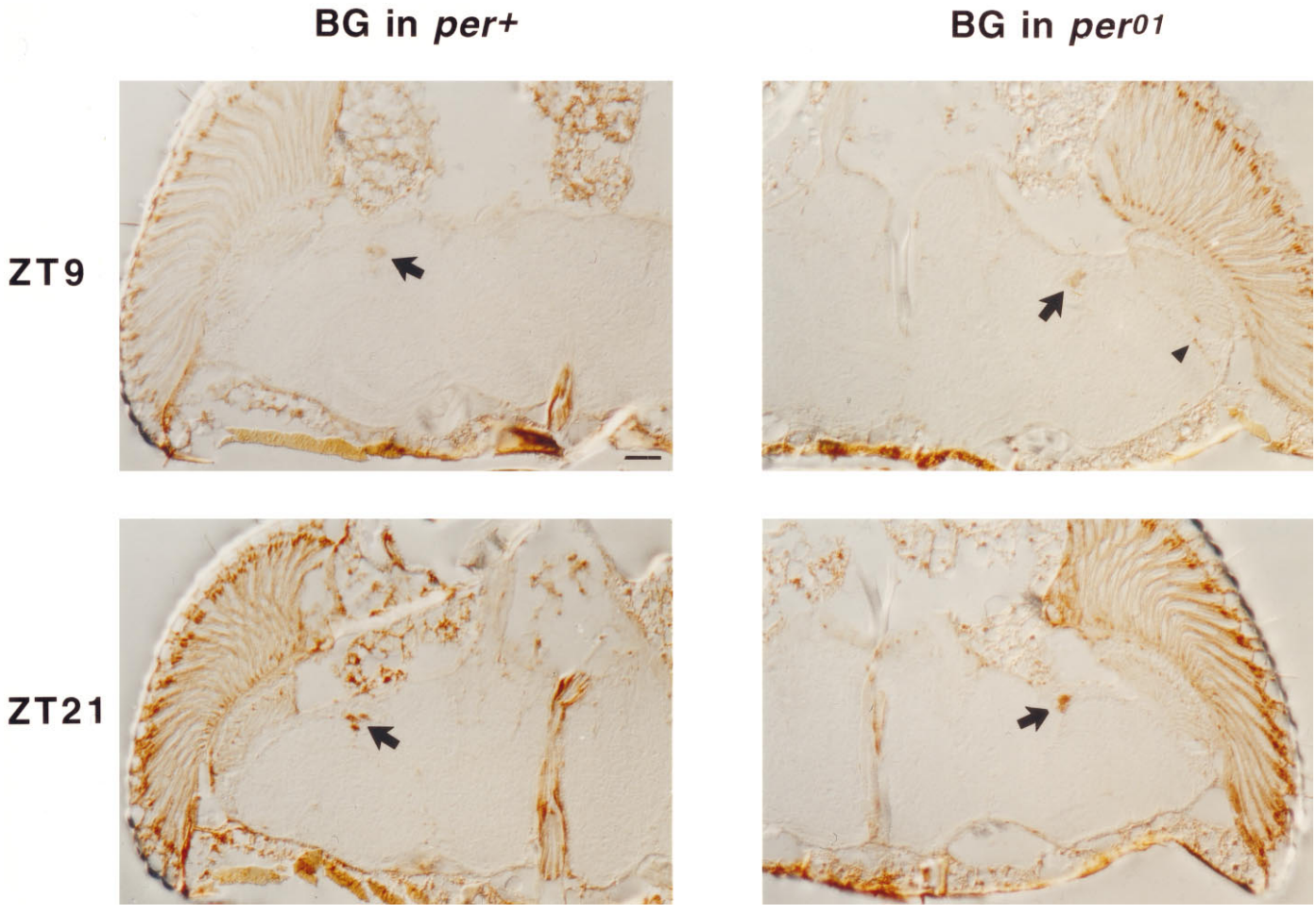


*Figure 9.* Temporal staining pattern of another BG transgenic strain. Males from the BG6 line (see Materials and Methods) for which the genetic backgrounds were either $per^{+}$ or $per^{01}$ were sectioned and stained with anti-β-GAL. In $per^{+}$, only weak staining of the $LN_v$ (*arrow*) and PRs was observed at ZT9. Staining in glia was nearly undetectable at this time point. At ZT21, strong staining in the $LN_v$ (*arrow*) and PRs, as well as weak staining in glia (in the lamina and bordering the medulla), can be observed. In $per^{01}$, only light staining of the $LN_v$ is observed at ZT9 (*arrow*). In contrast to the expression of BG6 in the $per^{+}$ background, there is also prominent staining in the nuclei of the PRs and glia cells (*arrowhead*). At ZT21, $LN_v$ are strongly labeled, whereas the signal intensities in the PRs and glia seem to be only slightly stronger compared with ZT9. Scale bar, 25 μm.

staining in SG flies (compare Figs. 2*A* and 3*C*). Strong glial staining was only observed along the outer rim of the medulla (Fig. 3*D*). In contrast to SG, only weak glial staining was observed in the lamina (Figs. 2*C* and 3*D*), the cortex, including neuropil borders (Figs. 2*A* and 3*C*), and the inner optic chiasm (Figs. 2*D* and 3*D*). Glial staining of BG transgenics therefore closely reflects PER expression in this cell type (cf. Ewer et al., 1992).

The nuclei of the PRs in BG flies showed robust reporter expression. The cytoplasm of the PR cells is also labeled but less strongly than in SG flies (Figs. 2*A*,*C*,*D*, 3*C*,*D*,*G*); this might contribute to the weaker signal in the lamina in BG flies (see above). Expression of the BG fusion protein in the thorax and abdomen was also inspected and found to be similar to that of PER (for an overview of *per*-expressing tissues in the whole fly, see Hall, 1995). As an example, nuclear BG staining in the outer layer of epithelial cells in an alimentary structure (the cardia) is shown (Fig. 3*H*).

The XLG fusion protein was expected to exhibit an expression pattern very similar to that of PER, because this transgene encodes nearly the full-length protein (Fig. 1). Yet the observed stainings in PR cells and glia were different from the wild-type and BG patterns, at least in terms of intensity of the signals (Fig. 4); XLG expression in the PRs is not restricted to the nucleus but is equally distributed through the whole cells (Fig. 4*E*). Whereas prominent glial expression was observed at the outer rim of the medulla in SG and BG, XLG flies showed very low expression in these cells (Fig. 4*A–C*). Moreover, these glial cells and few additional ones in the cortex of the optic lobe (Fig. 4*A*) were the only positively stained non-neuronal cells that we were able to identify (for example, no staining could be

←

or ZT of the preparations), using an intensity scale from 1 to 4. The means for each genotype are plotted as a function of ZT (see Materials and Methods, including the procedure of SEM calculation). *A*, Staining intensities in LNs in a $per^{+}$ background. *B*, $per^{01}$ background; in both genetic backgrounds, the staining intensities show circadian fluctuations, although cycling is less robust and with lower amplitude in the mutant background. *C*, Staining of glia in a $per^{+}$ background. *D*, $per^{01}$ background. Only in the $per^{+}$ background were strong circadian fluctuations of staining intensities detectable. *E*, PR staining in a $per^{+}$ background. *F*, $per^{01}$ background. Again, circadian changes in staining intensities were detectable only when $per^{+}$ was expressed.

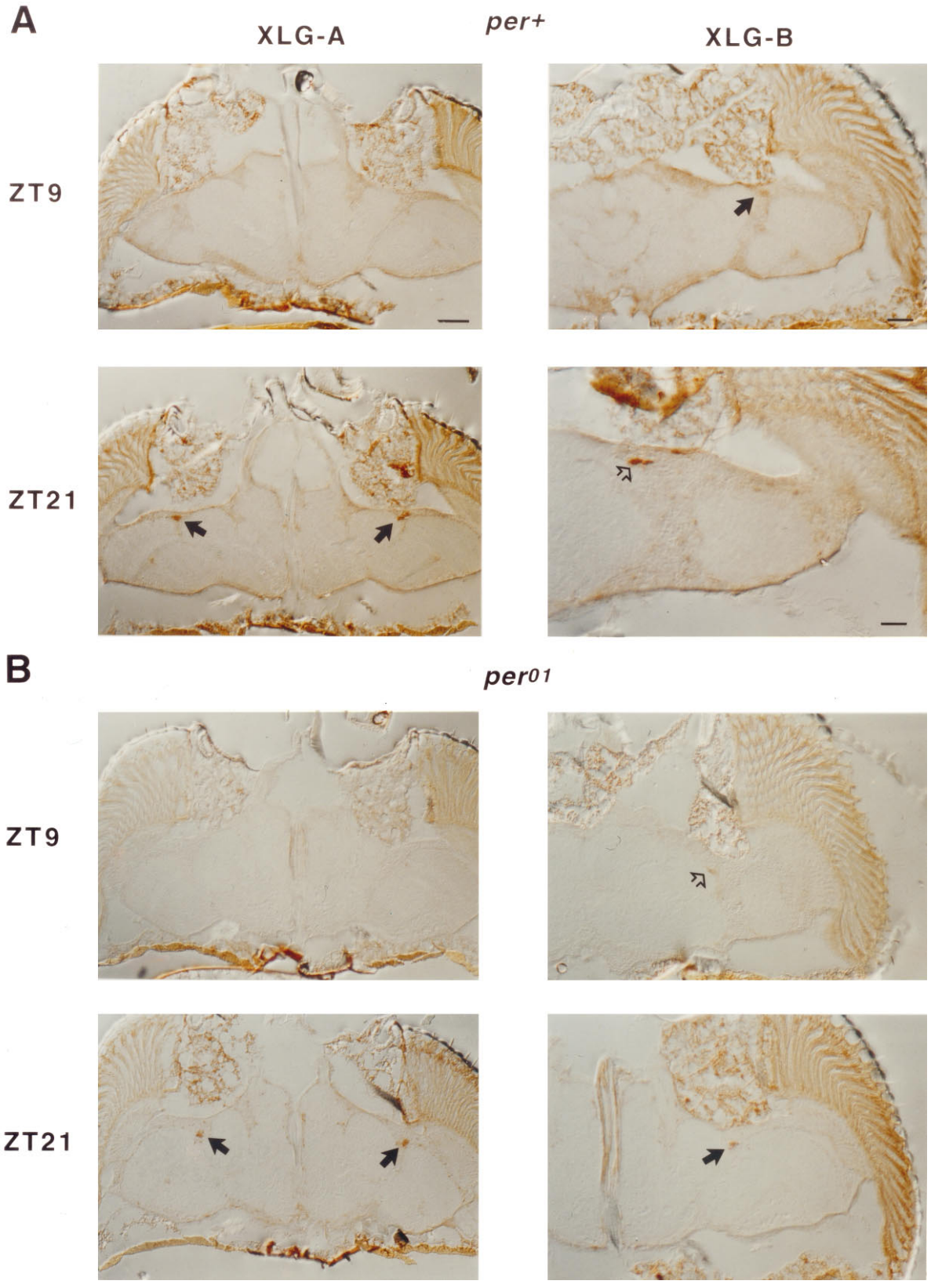


*Figure 10.* Temporal expression pattern of XLG transgenic flies. Males carrying the XLG construct (lines XLG-A and XLG-B) each with $per^{+}$ (*A*) or $per^{01}$ (*B*) were sectioned and stained with anti-β-GAL. *A*, In XLG-A, only weak cytoplasmic staining in the PRs is visible at ZT9. Scale bar, 40 μm. At ZT21, prominent staining in the $LN_v$ (*arrows*) is detectable, whereas staining in PRs seems only slightly increased compared with ZT9 and is mainly cytoplasmic. Glia staining at this high time point is just above the limit of detection. Magnification is as at ZT9. For the XLG-B line, similar expression patterns were observed. In $LN_v$ at ZT9, the signal was barely detectable (*solid arrow*), whereas prominent staining of the dorsal group of LNs ($LN_d$) appears at ZT21 (*open arrow*). Scale bars: ZT9, 25 μm; ZT21, 12.5 μm. *B*, In the $per^{01}$ background, no XLG-A-mediated (*Figure legend continues*)

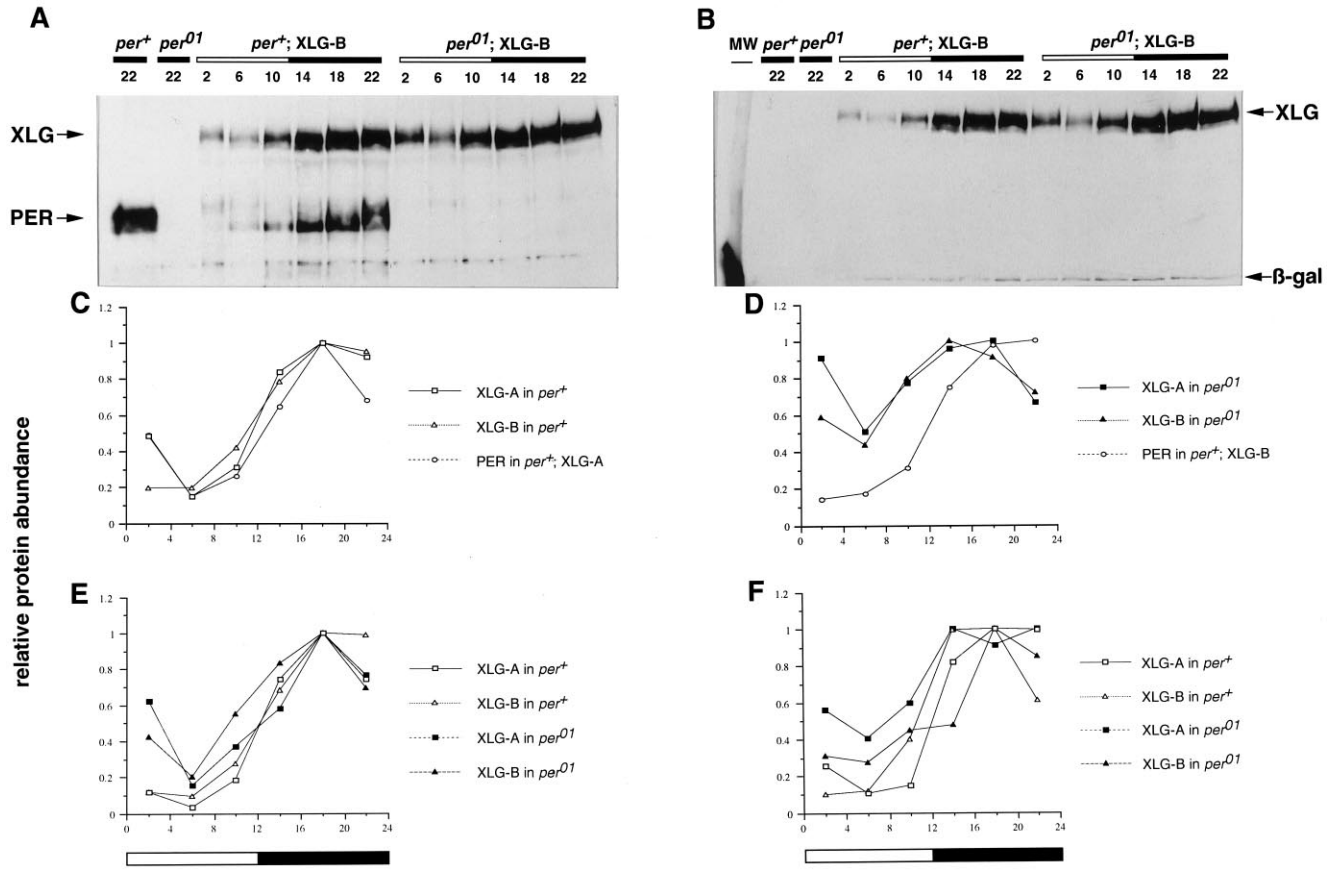


*Figure 11.* Western blots of XLG transgenics. Males carrying the A and B insert location of this fusion gene and either $per^+$ or $per^{01}$ had protein extracted from their heads, which was electrophoresed and subjected to immunoblotting as a function of ZT (i.e., different times within a 12:12 hr LD cycle when the adults were killed for protein extraction). These times are indicated above each lane in *A* and *B*. *B*, XLG-B based Western blots after incubation with polyclonal anti-PER antibody; in both $per^+$ and $per^{01}$ genetic backgrounds, the PER–β-GAL fusion protein undergoes similar changes in abundance and mobility as the endogenous PER protein does. For quantification of this experiment, see *C* and *D*. As controls, equal protein amounts of head extracts from *Df(1)w* ($per^+$) and $per^{01}$ $w$ $sn^3$ ($per^{01}$) flies were blotted on the same gel. Note the absence of endogenous PER in all genotypes for which the genetic background is $per^{01}$. *B*, Signals obtained after application of a monoclonal anti-β-GAL antibody [the same membrane (see *A*)] was stripped and subsequently incubated with this reporter-detecting reagent) and showed the same mobility shifts and fluctuations in abundance as in *A*, in both $per^+$ and $per^{01}$ genetic backgrounds. See *E* for quantification. In addition, a 116 kd protein band is detected by the anti-β-GAL antibody in all head extracts from the XLG transgenics but not in those from the two control strains. Note that this band runs at a similar position in the gel as does the bacterial β-GAL protein, which was included in the MW marker. *C–F*, Quantification of a set of Western blot experiments using a phosphoimager (see Materials and Methods). To allow amplitude and phase comparisons between different protein curves, the highest expression values for each protein in each experiment were set equal to 1. *C*, XLG-A and XLG-B proteins in the $per^+$ background. *D*, XLG-A and XLG-B in the $per^{01}$ background (for *C* and *D*, the proteins were detected with anti-PER). To compare the cycling of both fusion proteins with that of PER, endogenous PER abundance (from $per^+$ XLG-A flies in *C* and $per^+$ XLG-B flies in *D*) is also plotted. Amplitudes of protein cycling in these experiments were as follows: PER in XLG-A [strain B], 4 (6.5)-fold; XLG-A [B] in $per^+$, 4.5 (5)-fold; XLG-A [B] in $per^{01}$, 1.5 (2)-fold (for how the amplitudes were calculated, see Materials and Methods). For *E*, the same blots used to generate the data for *C* and *D* were subsequently incubated with anti-β-GAL (see above) and quantified; amplitudes were 11 (9.5)-fold for XLG-A [B] in the $per^+$ and 3.5 (3)-fold for XLG-A [B] in the $per^{01}$ background. In *F*, quantification of a second, independent Western blot experiment involving the XLG-A and XLG-B lines (in the $per^+$ and $per^{01}$ backgrounds) probed with anti-β-GAL was performed. Again, the XLG fusion proteins show robust abundance and mobility fluctuations in both genetic backgrounds (amplitudes for XLG-A [B] were 8 (9)-fold in the $per^+$ and 2 (3)-fold in the $per^{01}$ background. The *open bars* represent the light, and the *solid bars* the dark portion of the LD cycle, respectively.

detected in the lamina and the inner optic chiasm) (Fig. 4*C*,*E*). In contrast, XLG-mediated signals in *per*-expressing neurons were prominent and similar to those observed for BG. The XLG fusion protein also fills up the neuronal perikarya, making it possible to distinguish cell sizes and shapes. Figure 4, *A* and *B*, shows six cells of the $LN_d$ group. In addition, two large cells from the dorsal subset of the $LN_v$ are visible. Figure 4*D* illustrates staining of smaller DNs (diameter, ~3-5 μm) compared with the DNs shown in Figure 3*F* (diameter, ~8 μm). In both cases, these neurons (usually two) are located at similar lateral positions in the posterior dorsal brain and were the only DNs found in that region. This indicates that they belong to the

←

expression was detectable in LNs and glia at ZT9. As in $per^+$, there was only weak cytoplasmic PR staining at this time point. At ZT21, strong staining in the $LN_v$ (*arrows*) as well as in glia and PRs is visible. Magnifications are the same as for XLG-A ($per^+$). For the XLG-B line, similar signal fluctuations were observed, although weak staining of the $LN_d$ (*open arrow*) was detectable at ZT9. The *solid arrow* at ZT21 points to a group of $LN_v$ showing strong expression of the XLG-B fusion protein. Magnifications are as in XLG-B ($per^+$) at ZT9.

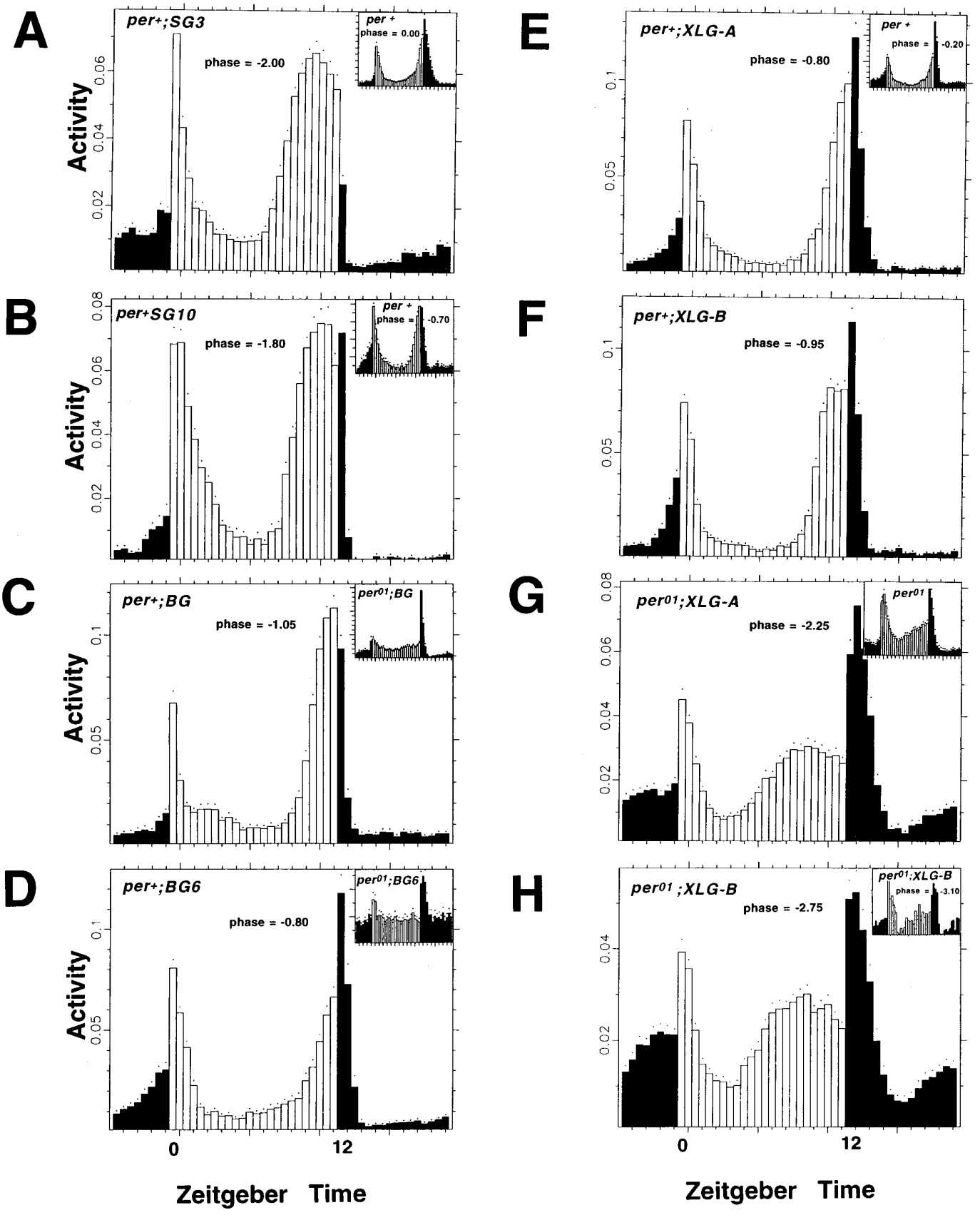


*Figure 12.* Locomotor activity of SG, BG, and XLG transgenics and their controls in LD cycles. Data were plotted from the entrainment portions (the first 7 or 14 d, 12:12 hr LD cycle) of the locomotor activity runs performed in this study (see Materials and Methods, Table 1). Histograms were generated by first superposing locomotor data from a given (male) fly (see *inset* in *H*), followed by superposing the daily activities of all flies (*Figure legend continues*)

**Table 1. Entrained and free-running behavior of SG, BG, and XLG transgenics**

| Genotype | No. of experiments (*n*) | Morning phase (hr ± SEM) | Evening phase (hr ± SEM) | Rhythmic/ tested (%) | Tau ± SEM |
|---|---|---|---|---|---|
| *per*$^{01}$ SG10/*Y*;*ry*$^{506}$ | 2 (13) | | | | |
| *w* SG10/*Y* | 2 (24) | +0.90 ± 0.1 | −1.80 ± 0.05 | 19/23 (82.6) | 22.3 ± 0.1 |
| *per*$^{01}$/*Y*;SG3;*ry*$^{506}$ | 3 (43) | | | | |
| +/*Y*;SG3;*ry*$^{506}$ | 3 (40) | +0.35 ± 0.1 | −2.00 ± 0.1 | 23/31 (74.2) | 23.8 ± 0.1 |
| *per*$^{01}$/*Y*;BG/TM2*ry*$^{506}$ | 2 (34) | | | | |
| +/*Y*;BG/TM2*ry*$^{506}$ | 2 (38) | +0.75 ± 0.05 | −1.05 ± 0.05 | 29/37 (76.3) | 23.7 ± 0.1 |
| *per*$^{01}$/*Y*;BG6;*ry*$^{506}$ | 2 (26) | | | | |
| +/*Y*;BG6;*ry*$^{506}$ | 2 (29) | +0.25 ± 0.1 | −0.80 ± 0.1 | 29/29 (100 ) | 23.3 ± 0.1 |
| *per*$^{01}$ *w sn*/*Y*;XLG-A | 3 (42) | −0.40 ± 0.1 | −2.25 ± 0.15 | 10/41 (24.4) | 24.6 ± 1.5* |
| *Df*(1)*w*/*Y*;XLG-A | 3 (47) | +0.35 ± 0.1 | −0.80 ± 0.1 | 42/46 (91.3) | 23.3 ± 0.1 |
| *per*$^{01}$*w sn*/*Y*;XLG-B | 3 (38) | −0.50 ± 0.1 | −2.75 ± 0.15 | 7/35 (20.0) | 21.9 ± 1.1* |
| *Df*(1)*w*/*Y*;XLG-B | 3 (46) | +0.20 ± 0.1 | −0.95 ± 0.1 | 43/45 (95.6) | 22.9 ± 0.1 |
| *w*/*Y* | 2 (13) | +0.05 ± 0.3 | −0.70 ± 0.1 | 13/13 (100 ) | 23.6 ± 0.1 |
| *Df*(1)*w*/*Y* | 5 (47) | +0.10 ± 0.15 | −0.20 ± 0.10 | 45/47 (95.7) | 23.6 ± 0.1 |
| +/*Y*;*ry*$^{506}$ | 6 (46) | +0.60 ± 0.1 | 0.00 ± 0.1 | 45/45 (100 ) | 24.1 ± 0.1 |
| Wild-type male (Canton S) | 1 (9) | −1.05 ± 0.2 | −0.50 ± 0.1 | 9/9 (100 ) | 23.8 ± 0.1 |

LD and DD behavior for the different transgenic types and controls. The latter carried a *per*$^{+}$ allele of the *period* locus, as well as marker mutations contained in the genetic backgrounds of the various transgenic types (see Materials and Methods). The two *per*$^{01}$ controls contained *ry*$^{506}$ or *w sn*$^{3}$ as marker mutations. All males tested from both strains ($n = 53$ for *per*$^{01}$*ry*$^{506}$ and $n = 30$ for *per*$^{01}$ *w sn*$^{3}$ were arrhythmic when tested under DD conditions. The second column shows the number of independent experiments that were done with the different transgenics during a time span of 18 months. *n* indicates the number of animals tested that entrained to the 12:12 hr LD cycle; these individual records were therefore used in the phase analysis. Note that not all animals entrained to this LD cycle; only between 65% (*per*$^{01}$ SG10/*Y*) and 97% (*per*$^{01}$ *w sn*/*Y*) of all the *per*$^{01}$ genotypes were rhythmic in LD. Overall, 86% of the flies among the 8 *per*$^{01}$ genotypes were rhythmic (i.e., had entrained). In contrast, 99% of all *per*$^{+}$-expressing males tested were rhythmic in these LD conditions. The morning and evening phase values were calculated from locomotor behavior recorded in the LD portion of the experiment using the Phase program (see Materials and Methods). Values (in hours) are given relative to lights-on (ZT0) for the morning phase and to lights off (XT12) for the evening phase. The last two columns tabulate the data collected in DD. The numbers of rhythmic individuals compared with the total tested (and the percentages), as determined by periodogram analysis (see Materials and Methods). From those analytical plots, "power" values are obtainable, as are the numbers of 0.5 hr time bins crossing the "significance line" (cf. Ewer et al., 1992) (see also Fig. 13). Only flies showing periods in combination with a power of ≥20 and a time-bin width of ≥2 were considered rhythmic. To determine whether the phase advances and period shortenings, observed in all transgenic strains in a *per*$^{+}$ background, were significant, nonparametric Mann–Whitney *U* tests were performed, comparing each P-element strain and its relevant control. In all cases, the observed differences were significant ($p < 0.05$).

*Although the average periods of the *per*$^{01}$ XLG-A or XLG-B flies were within the circadian range, the individual periods of the rhythmic flies were distributed over a broad range (between 18.5 and 27.5 hr for XLG-A and between 18 and 28 hours for XLG-B).

same group of cells that shows variable cell size rather than representing cells of two different groups, as was observed for the $LN_v$ (Fig. 3*C*,*D*). A different *group* of five to eight DNs expressing the BG fusion protein was found to be located in more central regions of the dorsal brain (data not shown).

The XLG fusion protein is present in the nucleus and the cytoplasm, and the majority of the signal seems to be in the latter compartment (Fig. 4*A–D*). This indicates that the C-terminal part of PER, not present in BG, is not responsible for proper nuclear localization of PER–β-GAL fusion proteins (see Discussion). We have no explanation for the relatively low expression of XLG in glia cells. Two independent transgenic lines (XLG-A and XLG-B) gave similar results, arguing against chromosomal position effects. Furthermore, Western blot experiments show that both transgenic lines express the fusion protein in comparable amounts to endogenous PER (see Fig. 11).

## Temporal pattern of transgene expression in *per*$^{+}$ and *per*$^{01}$ genetic backgrounds

The detailed analysis of the spatial expression patterns allowed us to study temporal changes in expression in the different cell types expressing the various fusion proteins.

To determine whether the different PER–β-GAL fusion proteins undergo PER-like circadian fluctuations in abundance, we performed X-gal and anti-β-GAL antibody stainings at different times of the day (see Materials and Methods). Flies were entrained for at least 3 d in 12:12 hr LD cycles before they were sectioned at a variety of ZTs. The transgene-mediated signals were also assessed in flies for

←

from the same genotype (for additional details about preparation of these plots, see Hamblen-Coyle et al., 1989). The *open bars* indicate activity exhibited in the light portion, and the *solid bars* activity monitored in the dark portion of the cycle. *A*, *per*$^{+}$ SG3 males ($n = 40$) and *ry*$^{506}$ control males ($n = 46$). *B*, *per*$^{+}$ SG10 males ($n = 24$) compared with their *w* control males ($n = 13$). Note the substantially earlier evening peak in SG transgenic flies. *C*, BG/*TM2* males in the *per*$^{+}$ ($n = 38$) and *per* $^{01}$ ($n = 34$) genetic backgrounds (the latter, *inset*). *D*, BG6 males in the same pair of backgrounds ($n = 29$ and 26, respectively). The phase advance (compared with the *ry*$^{506}$ control males shown in *A*) of the evening peak is not as strong as for SG (see also Table 1). Note as well that there is no anticipation of the LD and dark/light (DL) transitions in both of the *per* $^{01}$ BG strains. *E*, XLG-A males ($n = 47$) in a *per*$^{+}$ background showing only a subtle phase advance of their evening activity, compared with the control strain *Df(1)w* ($n = 47$) shown in the *inset*; XLG-A otherwise appeared to behave in a *per*$^{+}$-like manner. *F*, XLG-B in a *per*$^{+}$ background ($n = 46$), the behavior of which is very similar to that of *per*$^{+}$ XLG-A. *G*, *per* $^{01}$ XLG-A ($n = 42$). *H*, *per* $^{01}$ XLG-B ($n = 38$). Both *G* and *H* reveal complex patterns of LD behavior; the flies seemed to anticipate the LD changes, showing increased activity before the lights are turned off in the evening, with a distinct (not *per*$^{+}$-like) phase advance of nearly 3 hr. In addition, these *per* $^{01}$ XLG flies clearly reacted to LD and DL transitions as the straight *per* $^{01}$ *w sn*$^{3}$ control males do ($n = 30$; see *inset* in *G*). The complex behavior caused by the simultaneous presence of the XLG transgene and the *per* $^{01}$ allele was observed in the records from individual animals (see *inset* in *H*), and therefore is not a reflection of two subpopulations of differently behaving flies.

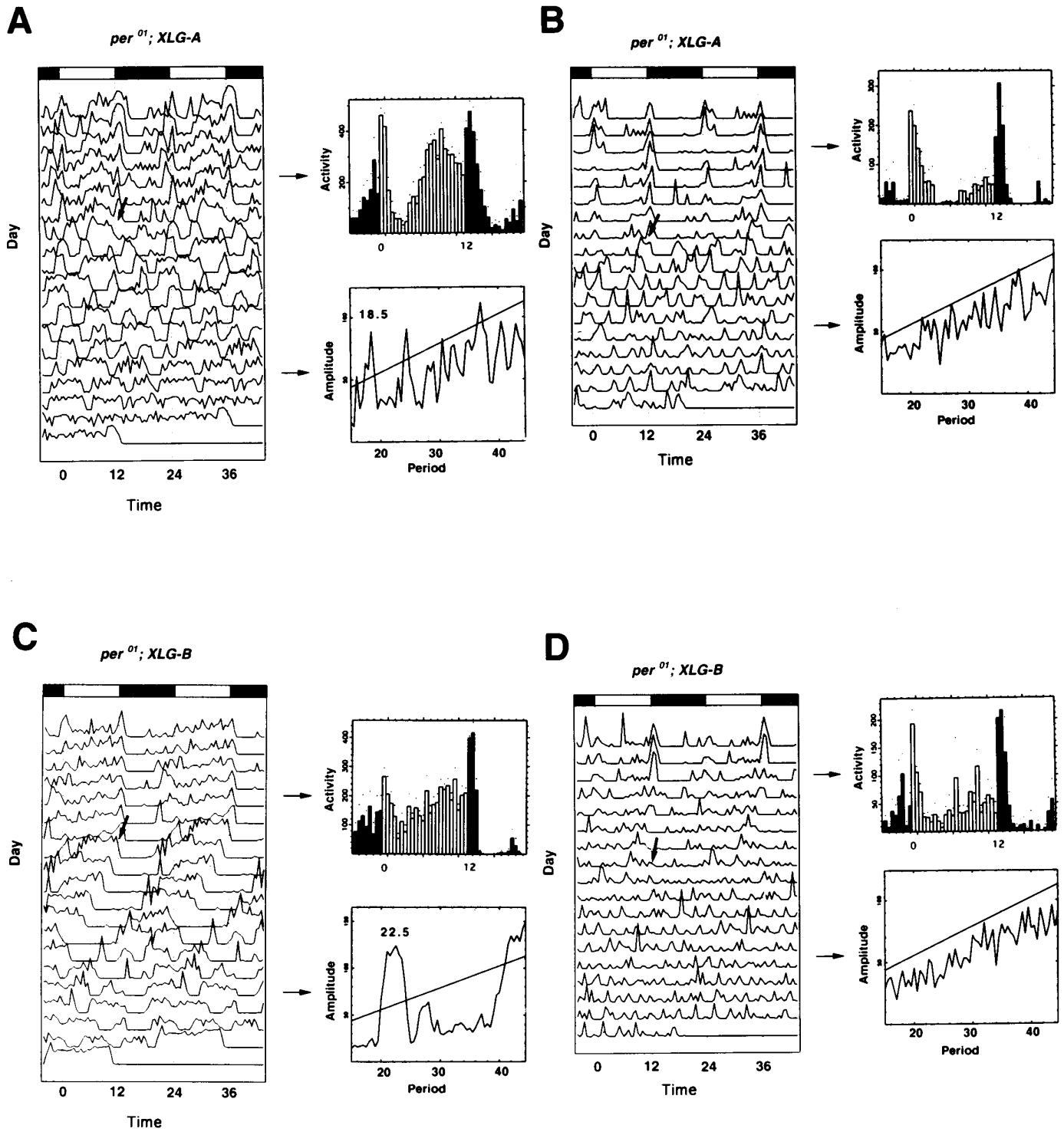


*Figure 13.* Entrained and free-running behavior of *per* $^{01}$ XLG flies. Rhythmic and arrhythmic individuals are exemplified. Each panel (in its *left* side) shows a double-plotted actogram (successive days of activity are displayed horizontally and vertically) for a fly that was monitored in 12:12 hr LD conditions for 7 d, followed by ≥10 d of additional monitoring in DD. The transition to DD is marked by an *arrow*. Activity plots (averaged per day; compare Fig. 12) for the time the fly was in LD accompany the actograms, as do plots of $\chi^2$ periodograms (Sokolove and Bushell, 1978; Hamblen et al., 1986) computed for the DD portion of the run. Peak values indicate the best estimate of the flies' free-running periods; the periodogram allows an estimation of the "power" (difference between the peak and the 5% significance line, measured in arbitrary units) and "width" (number of the 0.5 hr time bins at the sloping line that defines the 5% significant level). These metrics are indicators of the strength of a given fly's rhythm (cf. Liu et al., 1991; Ewer et al., 1992). *A*, A rhythmic *per* $^{01}$ XLG-A male, showing complex LD behavior, as depicted for the population average of this genotype (Fig. 12*G*); a power of 36.9 and a width of 4 classified this fly as rhythmic (period = 18.5). *B*, An arrhythmic *per* $^{01}$ XLG-A male. This individual was classified arrhythmic in this manner, because the power and width were each 1 where the $\chi^2$ line hit the 5% significance level. *C*, A rhythmic *per* $^{01}$ XLG-B male (period = 22.5) with a power of 63.8 and width of 9; the strength of this rhythm is close to that of wild-type flies (cf. Ewer et al., 1992). *D*, A *per* $^{01}$ XLG-B male, classified as arrhythmic in that the $\chi^2$ periodogram led to neither a positive power nor width value.

which only (endogenous) *per* gene was a loss-of-function mutation ($per^{01}$) to ask whether cycling could be controlled by the PER sequences in a given fusion protein.

It was reported that β-GAL enzyme activity shows circadian oscillations in head extracts of $per^+$ SG flies, whereas the activity was constant in a $per^{01}$ background (Zwiebel et al., 1991). Because this aspect of the study proved irreproducible (see Discussion), we performed X-gal stainings to reexamine this finding. When pairs of SG3 and SG10 transgenic flies, collected at opposite ZTs (ZT12 and ZT24), were stained in a $per^+$ background, no differences in staining intensities could be observed. At both time points, strong staining in PR and glial cells was observed, the only difference being a generally weaker signal in the $per^+$ SG10 flies (Fig. 5, *middle* and *bottom rows*). In contrast, PER protein shows its maximum abundance at ~ZT24 and at most ~20% of that expression level at ZT12 (Zerr et al., 1990; Zeng et al., 1994). Thus, the SG fusion protein (or at least its β-GAL activity) does not undergo circadian fluctuations after all. Note that in this regard it is possible to detect a mere twofold difference in *per* expression levels using X-gal staining on head sections of *per–lacZ* transgenics (Cooper et al., 1994) and that the PER protein cycles with a ~10-fold amplitude in biochemical experiments (Zeng et al., 1994). In agreement with the earlier study and as expected from the results just described, no cycling of the SG fusion could be detected in a $per^{01}$ background (Fig. 5, *top row*) (Zwiebel et al., 1991).

To quantify the staining data, sections of fly pairs with the same genotype, but opposite ZTs, were ranked blindly by three different observers (see Materials and Methods). After decoding these results, each pair was classified either as "equal staining at both ZTs," "higher staining at ZT24," or "higher staining at ZT12" (Fig. 6). Cycling seemed to occur only in one case (*open bar*), but this was in a $per^{01}$ background, and the phase was opposite to that of PER cycling in wild type. In all other cases, the majority of the pairs showed equal staining intensities at both time points (Fig. 6). We also performed anti-β-GAL antibody stainings at different ZTs on SG3 flies (in a $per^+$ genetic background); again, the results indicated noncycling (data not shown).

In the case of the BG fusion protein, oscillations in the reporter signals were clearly detectable in a $per^+$ background (Figs. 7–9). Strong staining in PRs, glia, and LNs was observed in BG/*TM2* flies at ZT3 and ZT21, whereas only weak signals in these tissues were observed at ZT9 and ZT15 (Fig. 7, *left column*). Interestingly, it seemed that the signal intensity in the LNs of $per^{01}$ BG/TM2 flies was also cycling; whereas prominent staining in the eyes and in glia was observed at all times, neuronal staining was clearly reduced at ZT9 (Fig. 7, *right column*). To confirm these observations, coded sections were scored blindly by three observers according to the strength of the staining signal in the three different *per*-expressing cell types. The result of this quantification revealed robust cycling in all three cell types in the $per^+$ genetic background (Fig. 8*A*,*C*,*E*) and appreciable (but relatively low-amplitude) fluctuations of LN expression in the $per^{01}$ background (Fig. 8*B*). The peaks of expression in all three cell types (in the $per^+$ background) were at ZT21 and ZT3, whereas the trough values were observed at ZT9 and ZT15. This is in good agreement with PER's immunohistochemically determined cycling in wild type; Zerr et al. (1990) reported peak expression at ~ZT24 and minimal expression at ~ZT12. In $per^{01}$, the weakest BG-mediated staining in the LNs was observed at ZT9; but in contrast to the results from $per^+$ BG flies, staining was again prominent at ZT15 (Figs. 7 and 8*B*). In PR and glia cells, the staining intensities in $per^{01}$ BG were constantly high (~three-fourths of the peak values from the $per^+$ flies) (Fig. 8*D*,*F*).

To ask whether fusion protein cycling apparently can be controlled by BG itself or is attributable to position effects (i.e., operating in the BG/*TM2* strain), additional experiments were performed using an independent transgenic line (BG6) in both $per^+$ and $per^{01}$ backgrounds. The fusion protein expression pattern was very similar to that described for BG/*TM2* except for the reduced number of glial cells that were stained in the BG6 line (compare ZT21 in Figs. 7 and 9). Temporal expression analysis revealed clear differences in staining intensity between flies sectioned at ZT9 and ZT21 (Fig. 9). In the $per^+$ background, staining was stronger at ZT21 in all three cell types (Fig. 9, *left column*). In $per^{01}$, cycling of the BG fusion protein was detectable in the LNs; in addition, and unlike what was observed in the experiments using the BG/*TM2* strain, the signal appeared to fluctuate in the PRs as well (Fig. 9, *right column*).

We conclude that the additional 230 amino acids present in BG are sufficient to drive rhythmic oscillations of that fusion protein in a PER-like manner. In a $per^+$ background, cycling seems to occur in the same cells and with similar phase as for PER fluctuations in wild-type flies. Cycling in a $per^{01}$ background is less robust and may be restricted to neurons; yet, the BG fusion protein fluctuates in a circadian fashion, independently of PER function.

To determine whether the additional *per*-coding sequences that are present in XLG flies influence protein cycling, the polypeptide encoded by this fusion gene was monitored temporally. First we stained sections from both XLG transgenic lines (XLG-A and XLG-B) at ZT9 and ZT21. As expected, a strong increase in staining intensity could be observed in the LNs late at night (Fig. 10*A*). Staining in the PRs was weak at ZT9 and increased only slightly at ZT21 (note also that the staining is not restricted to the PR nuclei; compare Fig. 4). Glial staining was not detectable at the low time point and was faintly visible at ZT21; this was expected, given the expression pattern of this transgene late at night (Fig. 4). In a $per^{01}$ background, cycling occurred in the LNs in both transgenic lines. In the weaker-expressing XLG-A line, no staining was detectable in the LNs at ZT9 (Fig. 10*B*). In contrast to the $per^+$ background, there appeared to be more robust fluctuations of staining intensity in the PRs; in addition, staining of glia in the outer rim of the medulla became clearly detectable at ZT21 (Fig. 10*B*, *bottom row*). Thus, it seems as if the general expression level might be higher in the mutant genetic background. The fact that this fusion protein consistently cycled in PR and glia cells in a $per^{01}$ background (in contrast to BG) suggests that the additional C-terminal sequences are necessary to achieve a rhythmic expression pattern that better reflects the wild-type pattern.

To quantify XLG-encoded protein levels, we performed immunoblottings with head extracts from both transgenic strains. XLG-A and XLG-B flies, carrying $per^+$ or $per^{01}$ in their genetic backgrounds, were collected at six different ZTs. Head protein extracts were separated on polyacrylamide gels. The ensuing Western blots, to which an anti-PER antibody was applied, were developed and the signals quantified (see Materials and Methods). This anti-PER reagent revealed circadian fluctuations of endogenous PER protein in abundance in both XLG transgenic lines. As has been reported for wild-type flies, maximum amounts of PER were detected between ZT18 and ZT22, and minimal levels were present between ZT6 and ZT10 (Fig. 11*A*,*C*,*D*) (cf. Zeng et al., 1994). Temporally dependent protein mobility shifts

were also observed, again as reported previously (Edery et al., 1994). These shifts are caused by phosphorylation; the faster-migrating form (~155 kDa) becomes phosphorylated, resulting eventually in the most slowly migrating one (~190 kDa) (Edery et al., 1994). In agreement with the earlier study, only the faster migrating form of PER is present at the beginning of the accumulating phase (ZT10–ZT14) (Fig. 11*A*). At ZT18, the first slower-migrating (phosphorylated) forms become visible, becoming predominant at ZT22. At ZT2, only the phosphorylated forms are present and at ZT6, both forms are present at very low levels (Fig. 11*A*).

The PER antibody also detected the XLG fusion protein, which is expressed at similar levels and shows circadian fluctuations in abundance as PER in both $per^+$ and $per^{01}$ genetic backgrounds (Fig. 11*A*,*C*,*D*). In addition to cycling with identical phase, the turnover of XLG occurs with a PER-like amplitude in a $per^+$ background (see legend to Fig. 11*C*,*D*). In contrast, the amplitude is reduced by >50% in a $per^{01}$ background (XLG-A, 1.5-fold; XLG-B, twofold) (Fig. 11*D*), indicating that endogenous PER is necessary to achieve full-amplitude cycling of the XLG fusion protein. The lower amplitude is attributable to higher protein concentrations at trough times of expression rather than lower levels at peak times (compare ZT2 and ZT6 of $per^+$ with the same $per^{01}$-based time points) (Fig. 11A). Mobility shifts of the XLG proteins were also detectable in both genetic backgrounds, similar to those described for PER (Fig. 11*A*). The shifts were not as drastic as observed for PER, perhaps because the resolution of small mobility differences for the ~300 kDa XLG fusion protein is not as good as for the smaller PER polypeptide. (However, the shifts were still obvious; compare ZT2 and ZT14 in Fig. 11*A*; the faster-migrating form is clearly absent at ZT2 in both genetic backgrounds.)

When the same blots were incubated with anti-β-GAL antibodies, similar fluctuations in abundance and mobility shifts of the fusion protein were observed (Fig. 11*B*). For unknown reasons, the amplitude of the molecular rhythm was higher in both genetic backgrounds, compared with those resulting from application of anti-PER (see legend to Fig. 11*E*). Nevertheless, the reduction of amplitude in the $per^{01}$ background was in the same range as observed with anti-PER antibody (>50%) (Fig. 11*E*), indicating that the differences obtained with both antibodies were only relative. To confirm these results, a second, independent experiment was performed using a different collection of flies and anti-β-GAL antibody. In this experiment, cycling in XLG-A (XLG-B) flies occurred with eightfold (ninefold) amplitude in $per^+$ and twofold (threefold) amplitude in a $per^{01}$ genetic background; thus, the amplitude reduction observed in a $per^{01}$ background is real (Fig. 11*F*).

In addition to the ~300 kDa XLG fusion protein band, a smaller ~116 kDa band was present in blots incubated with anti-β-GAL antibody. These smaller band comigrates with the actual *Escherichia coli* β-GAL protein, included as a molecular weight marker (Fig. 11*B*). Because this band is present in all lanes containing extracts from XLG transgenic flies, but absent in $per^+$ and $per^{01}$ control flies, it is very likely derived from the fusion protein. It is possible that the 116 kDa band is a degradation product resulting from the cyclical turnover of the PER–β-GAL fusion protein. As expected from the long half-life of β-GAL activity in *Drosophila* (Monsma et al., 1988), no daily fluctuations of its abundance could be observed (Fig. 11*B*; also data not shown). Note also that the relatively small polypeptide is more abundant than suggested by the blot shown in Figure 11*B*; to transfer the large XLG proteins quantitatively, unusually long protein transfers were necessary, resulting in a substantial loss of the smaller β-GAL protein (data not shown) (see also Materials and Methods). High amounts of this protein are usually present in protein extracts of flies carrying fusion genes encoding PER–β-GAL fusion proteins that undergo circadian fluctuations (e.g., in BG flies). In contrast, in transgenics for which the fusion proteins do not cycle the relative abundance of β-GAL is much lower (e.g., SG), indicating that rhythmic fluctuations of PER–β-GAL fusion proteins result in increased amounts of free β-GAL, probably attributable to circadianly regulated protein degradation (Dembinska et al., 1997).

Given these results, the anti-β-GAL antibody stainings might not reveal the intracellular distribution of the fusion proteins, because the observed staining patterns probably result from detection of both the intact fusion proteins and β-GAL, which would not necessarily be co-localized. To address this matter, we performed stainings of BG and XLG flies (in which the β-GAL is abundant on Western blots) with anti-PER antibodies in a $per^{01}$ mutant background, detecting only the intact fusion proteins. $per^{01}$ XLG-B males were stained at ZT15 ($n = 4$) and ZT21 ($n = 4$) and $per^{01}$ BG/TM2 males at ZT16 ($n = 3$) and ZT20 ($n = 2$), respectively. The results of these preliminary experiments indicate that the fusion proteins were present in both the cytoplasm and the nucleus at times when staining should be restricted to either one of these compartments (cytoplasmic at ZT15/ZT16, nuclear at ZT20/ZT21) (Curtin et al., 1995). Therefore, we conclude that the anti-β-GAL stainings performed in this study reflect (at least qualitatively) the intracellular distribution of the intact BG and XLG fusion proteins and that this distribution is different from that of PER; for example, the fusion proteins do not exhibit obvious circadianly regulated shifts from the cytoplasm into the nucleus (cf. Curtin et al., 1995).

## Locomotor activity behavior

To test whether the observed cycling or noncycling of the different *per–lacZ* fusion proteins has biological consequences, we studied the locomotor activity of $per^+$ and $per^{01}$ flies that carried either an SG, BG, or XLG transgene. Because the histological and immunoblot experiments were performed exclusively on flies kept under LD cycling conditions (see above), we focused especially on the locomotor behavior recorded from (male) flies kept under the same 12:12 hr LD regime. In LD, wild-type flies show increasing locomotor activity before lights on in the morning and especially before lights off in the evening, whereas $per^{01}$ flies simply react to the environmental changes by increasing their activity after the lights go on or off (Hamblen-Coyle et al., 1992; Wheeler et al., 1993) (Fig. 12*A*,*G*, *insets*).

## SG and BG transgenics

As expected, both SG transgenic lines showed clear anticipation of the morning and evening light transitions when tested in the $per^+$ background (Fig. 12*A*,*B*). The phase of the morning activity peak was in both cases in the range of the wild-type controls. Interestingly, the phase of the evening peak differed significantly from control values in both SG3 and SG10; the transgenics' phase for the evening activity peak was 2.0 and 1.1 hr earlier, respectively, when compared with the relevant controls (Fig. 12*A*,*B*; Table 1).

The two BG transgenic lines exhibited a behavior similar to that just described for SG. In the $per^+$ background, BG flies anticipated the environmental changes and also showed an earlier than normal phase of the evening peak. The phase advance associated

with the BG-*lacZ* transgene was not as extreme as in SG, being 1.1 hr (BG/*TM2*) and 0.8 hr (BG6) earlier compared with the wild-type controls; but the transgenics values were still significantly different from the controls (Fig. 12*C*,*D*; Table 1). The fact that all SG and BG transgenic strains tested manifest a clear phase advance of their evening activity peaks shows that these fusion proteins influence behavior, possibly by interfering with the product of the endogenous *per* gene or with a PER protein partner (cf. Vosshall et al., 1994; Gekakis et al., 1995; Zeng et al., 1996). The cyclical expression of the BG fusion protein, in contrast to SG's temporal constancy, might explain BG's milder impact on behavior.

Despite the fact that both the SG and BG transgenics manifest significant phase advances of their evening activity peaks, their free-running locomotor activity periods were close to that of the relevant controls. Under DD conditions, the periods of SG10 and SG3 transgenic flies were 1.3 and 0.3 hr shorter compared with their controls (the difference was significant) (Table 1). In the case of BG/*TM2* and BG6, periods were significantly shortened by 0.4 and 0.8 hr, respectively, compared with the period of the $per^+$ ($ry^{506}$-marked) control (Table 1). These weak effects on free-running behavior contrast with those of the $per^S$ mutation; compared with wild-type, this mutant shows a phase advance of 2.6–2.9 hr (Hamblen-Coyle et al., 1992), similar to the earlier than normal evening peak in $per^+$ SG flies (Table 1); but $per^S$'s free-running locomotor activity period is 5 hr shorter than normal (Konopka and Benzer, 1971).

SG and BG transgenics did influence wild-type free-running behavior in addition to the mild period-shortening effects; only ~70-80% of the two SG transgenics and the BG/*TM2* flies were rhythmic in a $per^+$ genetic background, whereas in all the $per^+$ controls, 100% of the individuals were rhythmic (Table 1). The transgenes' impact on normal behavior was especially prominent in one experiment, in which the flies were kept for 14 d in LD (instead of 7 d in all other experiments) before the transition to DD occurred. In this prolonged behavioral test, 43% of the SG3 transgenics and 56% of the BG/*TM2* flies were arrhythmic in DD, suggesting that older flies are more sensitive to the presence of the SG and BG fusion proteins. SG10 and BG6 transgenics were only tested after 7 d of LD entrainment, and their percentages of rhythmicity in subsequent DD were 83 and 100%.

In a $per^{01}$ background, SG3 and SG10 transgenic flies did not anticipate the LD transitions and, like the $per^{01}$ controls, showed increases in locomotor activity that seemed to be mere responses to the environmental transitions (data not shown) (Fig. 12*G*, *inset*). In the same mutant background, the BG fusion protein is rhythmically expressed in the *per* LNs in both BG transgenic strains (see above); and rhythmic expression of the complete PER protein (encoded by a promotorless 7.2 kb genomic *per* construct) in these pacemaker neurons is sufficient to restore free-running rhythmic locomotor behavior in $per^{01}$ flies (Frisch et al., 1994). However, no such (behavioral) rescue was observed in the case of the two lines transformed with the BG construct. As was found for SG, both BG/*TM2* and BG6 flies simply reacted to the environmental changes (Fig. 12*C*,*D*, *insets*). Thus, rhythmic expression of the truncated, β-GAL-carrying PER protein is not sufficient to restore normal LD behavior to the arrhythmic $per^{01}$ mutant.

As expected from these results, both SG and BG transgenic strains also did not rescue arrhythmic locomotor activity behavior under free-running (DD) conditions; all animals that were tested under these conditions were as arrhythmic as the $per^{01}$ controls (Table 1).

## XLG transgenics

In contrast to the SG and BG transgenic types described above, the XLG transgene encodes for the whole PER protein with exception of the last 10 amino acids (see Materials and Methods). Here, the rhythmic expression of this PER–β-GAL fusion protein in both $per^+$ and $per^{01}$ backgrounds (see above) is correlated with the behavioral results; $per^+$ XLG flies, tested under LD conditions, anticipated the light regime changes in the morning and evening, as normal flies do. But, as noted previously for the SG and BG strains, the XLGs showed a phase advance of the evening activity peak of 0.6 hr (XLG-A) and 0.8 hr (XLG-B), respectively, compared with the control flies (Fig. 12*E*,*F*; Table 1). This difference was significant for both XLG lines (see legend to Table 1). These mild phase advances (in LD conditions) were loosely correlated with an effect on free-running behavior; the periods observed under DD were 0.3 hr (XLG-A) and 0.7 hr (XLG-B) shorter than in the $per^+$ (nontransgenic) control. (Both strains were in fact significantly different from *Df(1)w* control; see Table 1.) In addition, a mild impact on general rhythmicity was observed in one of these strains; 91% of the XLG-A flies were rhythmic under free-running conditions (Table 1).

To determine whether the XLG transgenics could restore rhythmic behavior in $per^{01}$ flies, we first tested the locomotor activity behavior of $per^{01}$ XLG in LD conditions; wild-type-like anticipations of the environmental changes were observed in both of the XLG lines (in XLG-A flies, however, only anticipation of the LD transition in the evening was observed) (Fig. 12*G*). Interestingly, the phase of the evening peaks was even more advanced than it was for the same transgenes in a $per^+$ background: 2.1 hr earlier for $per^{01}$ XLG-A and 2.6 hr earlier in the case of $per^{01}$ XLG-B (Fig. 12*G*,*H*; Table 1). In addition, these transgenic adults showed a second and rather striking increase in locomotor activity just after the lights went on in the morning and off again in the evening; this is what occurs in $per^{01}$ (Fig. 12*G*,*H*). Therefore, it appears as if the LD behavior of $per^{01}$ flies, influenced by the XLG transgene, consists of two components: a "rescued" component, revealed by the anticipation of (at least) the LD transition, and a "mutant" component, reflected by the prominent reaction to the LD and LD transitions. It is important to note that these complex behavioral patterns were observed for individual flies (Figs. 12*H*, *inset*, 13) and are not a reflection of two XLG subpopulations in a given experiment (one acting quasi-normally, the other acting like $per^{01}$).

The LD behavior of the $per^{01}$ XLG flies just described is most likely the result of the weak, hence, incomplete rescue that was effected by the XLG transgenes. This was also concluded from analyzing the free-running behavior of $per^{01}$ mutants carrying this *per–lacZ* construct. Only 24% of the $per^{01}$;XLG-A and 20% of the $per^{01}$;XLG-B males tested were significantly rhythmic in DD (e.g., Fig. 13), with average periods of ~25 and 22 hr, respectively. The variations in these mean values were large (Table 1). Reasons that might explain the poor rescue qualities of this fusion protein are discussed below.

## DISCUSSION

The spatial expression of the SG, BG, and XLG fusion proteins is mainly restricted to *per*-expressing cells or to a subset of them. Only the SG transgenics show expression in some glia cells that have not been described to express *per* (Fig. 2). A reason for detection of these additional cells might be the generally higher expression level (compared with PER) of SG in glia cells; thus, these cells could express *per* in wild-type but were not identified in

anti-PER antibody stainings owing to naturally low expression levels. It is not known why SG appears at relatively low levels in the LNs; a possible explanation is that this fusion protein is distributed throughout the neurons, including nucleus, soma, and axonal processes. Nevertheless, expression in SG neurons is likely to be reduced, compared with the strong expression in the PR cells, in which the signal is indeed spread through the cells and their processes (Fig. 2). Expression of the BG fusion protein most closely reflects the spatial expression pattern of PER as well as its staining intensity in the different cell types.

The prominent BG expression in *per* neurons at ZT21 is not restricted to the nucleus, indicating that the intracellular localization of this fusion protein does not reflect that of PER (cf. Curtin et al., 1995). This difference is not the result of free β-GAL in addition to the full-length fusion protein, because anti-PER stainings of transgenics (in a $per^{01}$ background) gave similar results. Because the XLG fusion protein shows the same intracellular distribution as BG, the failure to move completely into the nucleus is not attributable to the missing one-third of PER residues in the latter. Instead, we suggest that the β-GAL portion of the fusion protein interferes with the ability to translocate efficiently into the nucleus, probably by faulty protein–protein interactions.

All three fusion genes analyzed in this study contain the PAS domain, shown to be an important element for PER–TIM dimerization (Gekakis et al., 1995). The PER–TIM complex is present between ZT16 and ZT20, and the whole complex shifts into the nucleus at ~ZT18 (Lee et al., 1996; Zeng et al., 1996). Removal of either PER or TIM from the complex leads to predominantly cytoplasmic distribution of the respective partner (Vosshall et al., 1994; Hunter-Ensor et al., 1996; Myers et al., 1996). The SG fusion protein is located in the cytoplasm of PR and glia cells of $tim^{01}$ flies; it is partly nuclear in $tim^{+}$, indicating that SG, and therefore probably the bigger BG and XLG fusion proteins as well, can interact with the *tim* gene product (Fig. 2) (Vosshall et al., 1994). Nevertheless, these putative interactions are not sufficient to translocate the fusion proteins into the nucleus efficiently. The mobility shifts we observed suggest that the XLG fusion protein is phosphorylated in a PER-like manner. This makes it unlikely that increasing phosphorylation is crucial for nuclear entry; thus, other mechanisms would be disrupted with respect to the fusion proteins' subcellular behavior.

The SG fusion protein is expressed in a constant manner. Yet, it has been reported that the β-GAL activity of this protein cycles in a $per^{+}$ background (Zwiebel et al., 1991). This previous observation was incorrect (Fig. 5) (Dembinska et al., 1997). The mRNA coding for the SG protein does undergo *per*-like circadian fluctuations (Zwiebel et al., 1991), suggesting that the protein is synthesized in a periodic manner. The fact that we observe constant SG protein expression is probably attributable to the missing PER sequences in SG; that is, the absence of C-terminal residues make this protein more stable than PER.

The BG fusion protein, which contains an additional 230 amino acids, cycles in both genetic backgrounds in the LNs, and in PR and glia cells in $per^{+}$. The robust cycling observed in a $per^{+}$ background implicates the following two features of the BG fusion gene: (1) its RNA should cycle (as does the shorter SG fusion transcript), which could contribute to rhythmic expression of the protein, and (2) the BG protein must be able to turn over in a PER-like manner, owing to the additional 230 amino acids (compared with SG). These residues seem to contain sequences that permit the fusion protein to be degraded in a relatively rapid manner, such that its half-life is short enough for the protein to exhibit troughs in its cycling (cf. Wood, 1995). For example, BG contains two possible PEST sequences, whereas SG contains only one. (PER contains four possible PESTs, which are all included in the XLG construct; Fig. 1.) PEST sequences have been implicated in fast protein degradation (Rogers et al., 1986) and do seem to function in this manner in *Drosophila* (Belvin et al., 1995).

That BG cycles in a $per^{01}$ background indicates some *per*-independent function of this protein. But why is it cycling less robustly and only in the LNs? The fact that BG is expressed at high levels in all other cells throughout the circadian cycle suggests that the molecular feedback loop, in which PER is thought to repress its own transcription (Hardin et al., 1990), is not functional in $per^{01}$ BG flies. Indeed, no RNA cycling could be observed in $per^{01}$ flies transformed with a BG–luciferase transgene (R. Stanewsky, unpublished observations). The BG protein cycling in LNs therefore is most likely a consequence of rhythmic protein degradation in these cells. One factor responsible for this turnover might be the light-induced degradation of the TIM protein (Hunter-Ensor et al., 1996; Lee et al., 1996; Myers et al., 1996; Zeng et al., 1996). TIM continues to cycle (with a low amplitude) in a $per^{01}$ background under LD conditions (Zeng et al., 1996); this is probably the driving force for the BG turnover in that mutant background, given that TIM is necessary to stabilize PER. It is also possible that the molecular feedback loop is functional only in the LNs and that rhythmic RNA expression remained undetected because the majority of transcripts (in PRs and glia) do not cycle. In any case, our results indicate another special feature of the LNs (cf. Frisch et al., 1994): these cells uniquely allow this PER fusion protein to undergo daily oscillations in its abundance.

The XLG fusion protein cycles robustly (Figs. 10, 11). In contrast to BG, it also cycles in PR and glia cells in a $per^{01}$ background, which might explain the high amplitude of cycling observed in Western blots. A reason for the robust (PER-independent) cycling could be that XLG is more degradable because of the additional C-terminal sequences, which include two additional PEST sequences (including the most conserved one; see Fig. 1). But the fact that both BG and XLG show the same robust cycling in our histochemical experiments in a $per^{+}$ background and that XLG (in $per^{+}$) cycles with the same amplitude as endogenous PER (Fig. 11) indicate that both fusion proteins are equally degradable. This suggests that the robust cycling of XLG (compared with BG) in a $per^{01}$ background is attributable to functional elements associated with the additional amino acids contained in XLG, which allow this protein to regulate its own transcription and, therefore, be synthesized in a rhythmic manner. We therefore expect that XLG RNA cycles in a $per^{01}$ background and, given the PER-like temporal mobility shifts, believe that this transgene can at least partially fulfill PER's function in the molecular feedback loop.

Consistent with this hypothesis, XLG is able to mediate a biological clock function in $per^{01}$ flies, although only in a mediocre manner (Figs. 12, 13). The behavioral phase advances observed for $per^{01}$;XLG flies (Table 1) indicate that XLG is not able to control locomotor behavior properly. This is also indicated by the prominent $per^{01}$-like increase of locomotor behavior observed in the same individuals at the times of LD transitions (cf. Wheeler et al., 1993). The same has been observed in certain other *per* mutants associated with weak clock function, such as $per^{L}$ (cf. Dowse and Ringo, 1987). $per^{L}$ flies show a prominent increase in locomotor activity after the environmental transitions, in addition to their characteristic evening activity peak 5–6 hr after the lights

go off (Hamblen-Coyle et al., 1992). Thus, one aspect of "strong" clock function (newly revealed here) is to suppress the rapid increases in locomotion that accompany these environmental transitions.

As expected from the LD behavior of XLG flies, only a low percentage of these transgenic individuals showed rhythmic behavior under free-running conditions; the periods were spread over a wide range and were associated with a weak overall rhythmicity (Figs. 12*G*,*H*, 13; Table 1).

Two possibilities could explain the poor rescue qualities of the XLG construct. First, the XLG protein, although it exhibits most of the PER attributes thought to be important in establishing a molecular feedback loop, may possess anomalies (inadequacies, or malfunctions, stemming from the fused β-GAL part of the protein or the C-terminal truncation) that lead to a poor function of that loop. Second, XLG may function well to establish the cycling molecular oscillator but functions subnormally in regulating clock-controlled genes (genes for which the expression cycles are *per*-dependent and may be within output pathways to locomotor behavior) (for review, see van Gelder and Krasnow, 1996).

All three fusion proteins influenced normal locomotor behavior (Fig. 12; Table 1), indicating that they interfere with the endogenous PER protein function. During the accumulating phase of the PER–TIM complex (between ZT16 and ZT20), twice as much TIM as PER is present in head extracts (approximately half of it bound to PER), indicating that there is a substantial amount of free TIM present at this cycle-time (Zeng et al., 1996). Because the fusion proteins probably interact quasi-normally with TIM (see above), it is possible that in $per^+$ SG, BG, or XLG flies, the sum of PER–TIM and SG/BG/XLG–TIM complexes is at higher level than that of PER–TIM complexes in wild-type flies. In other words, biological relevant complex concentration would be reached earlier in the transgenic flies compared with genetically normal ones. The earlier accumulation of TIM complexes could cause the phase advances and period shortenings that were observed in the transgenics. This hypothesis can also explain why the phase advances in SG flies are more substantial compared with BG and XLG. SG does not cycle and does not have to undergo a rise in its level to form an inappropriately high concentration of SG–TIM complexes. These phenomena and suppositions could be related to the fact that extra copies of functional *per* alleles result in period shortenings (Smith and Konopka, 1982; Rutila et al., 1992).

In summary, our study has allowed us to map certain functions of *per* to specific sequences of this clock gene. The fusion gene containing the smallest amount of *per* gives a quasi-normal spatial expression, but the fusion protein is not expressed in a rhythmic manner. The fusion containing an additional 230 amino acids exhibits a normal spatial expression pattern, and this protein undergoes PER-like circadian changes in abundance in *per*-expressing cell types, which occur independent of PER in the LNs. The fusion gene containing nearly all of *per*'s coding sequence shows rhythmic expression in all *per*-expressing cells, independent of $per^+$'s presence. Uniquely, the expression of this fusion gene's products is correlated with rhythmic behavior, including that of flies otherwise lacking a functional form of *per*.

## REFERENCES


Belvin MP, Jin Y, Anderson KV (1995) Cactus protein degradation mediates *Drosophila* dorsal-ventral signaling. Genes Dev 9:783–793.

Burbach KM, Poland A, Bradfield CA (1992) Cloning of the Ah-receptor cDNA reveals a distinctive ligand-activated transcription factor. Proc Natl Acad Sci USA 89:8185–8189.

Citri Y, Colot HV, Jacquier AC, Yu Q, Hall JC, Baltimore D, Rosbash M (1987) A family of unusually spliced biologically active transcripts encoded by a *Drosophila* clock gene. Nature 326:42–47.

Cooper MK, Hamblen-Coyle MJ, Liu X, Rutila JE, Hall JC (1994) Dosage compensation of the *period* gene in *Drosophila melanogaster*. Genetics 138:721–732.

Curtin KD, Huang ZJ, Rosbash M (1995) Temporally regulated nuclear entry of the *Drosophila period* protein contributes to the circadian clock. Neuron 14:365–372.

Dembinska ME, Stanewsky R, Hall JC, Rosbash M (1997) Circadian cycling of a *period-lacZ* fusion protein in *Drosophila*: evidence for an instability cycling element in PER. J Biol Rhythms, in press.

Dowse HB, Ringo JM (1987) Further evidence that the circadian clock in *Drosophila* is a population of coupled oscillators. J Biol Rhythms 2:65–76.

Dushay MS, Rosbash M, Hall JC (1992) Mapping the *Clock* rhythm mutation to the *period* locus of *Drosophila melanogaster* by germline transformation. J Neurogenet 8:173–179.

Edery I, Zwiebel LJ, Dembinska ME, Rosbash M (1994) Temporal phosphorylation of the *Drosophila* period protein. Proc Natl Acad Sci USA 91:2260–2264.

Ewer J, Frisch B, Hamblen-Coyle MJ, Rosbash M, Hall JC (1992) Expression of the *period* clock gene within different cell types in the brain of *Drosophila* adults and mosaic analysis of these cells' influence on circadian behavioral rhythms. J Neurosci 12:3321–3349.

Frisch B, Hardin PE, Hamblen -Coyle MJ, Rosbash M, Hall JC (1994) A promotorless *period* gene mediates behavioral rhythmicity and cyclical *per* expression in a restricted subset of the *Drosophila* nervous system. Neuron 12:555–570.

Gekakis N, Saez L, Delahaye-Brown A-M, Myers MP, Sehgal A, Young MW, Weitz CJ (1995) Isolation of *timeless* by PER protein interactions: defective interaction between *timeless* protein and long-period mutant $PER^L$. Science 270:811–815.

Hall JC (1995) Tripping along the trail to the molecular mechanisms of biological clocks. Trends Neurosci 18:230–240.

Hamblen MJ, Zehring WA, Kyriacou CP, Reddy P, Yu Q, Wheeler DA, Zwiebel DJ, Konopka RJ, Rosbash M, Hall JC (1986) Germline transformation involving DNA from the *period* locus in *Drosophila melanogaster*: overlapping genomic fragments that restore circadian and ultradian rhythmicity to $per^0$ and $per^-$ mutants. J Neurogenet 3:249–291.

Hamblen-Coyle MJ, Konopka RJ, Zwiebel LJ, Colot HV, Dowse HB, Rosbash M, Hall JC (1989) A new mutation at the *period* locus of *Drosophila melanogaster* with some novel effects on circadian rhythms. J Neurogenet 5:229–256.

Hamblen-Coyle MJ, Wheeler DA, Rutila JE, Rosbash M, Hall JC (1992) Behavior of period-altered rhythm mutants of *Drosophila* in light:dark cycles. J Insect Behav 5:417–446.

Hardin PE, Hall JC, Rosbash M (1990) Feedback of the *Drosophila period* gene product on circadian cycling of messenger RNA levels. Nature 343:536–540.

Hardin PE, Hall JC, Rosbash M (1992) Circadian oscillations in period gene mRNA levels are transcriptionally regulated. Proc Natl Acad Sci USA 89:11711–11715.

Helfrich-Förster C (1995) The period clock gene is expressed in central nervous system neurons which also produce a neuropeptide that reveals the projections of circadian pacemaker cells within the brain of *Drosophila melanogaster*. Proc Natl Acad Sci USA 92:612–616.

Helfrich-Förster C, Homberg U (1993) Pigment-dispersing hormone-immunoreactive neurons in the nervous system of wild-type *Drosophila melanogaster* and of several mutants with altered circadian rhythmicity. J Comp Neurol 337:177–190.

Huang ZJ, Curtin KD, Rosbash M (1995) PER protein interactions and temperature compensation of a circadian clock in *Drosophila*. Science 267:1169–1172.

Hunter-Ensor M, Ousley A, Sehgal A (1996) Regulation of the *Drosophila* protein timeless suggests a mechanism for resetting the circadian clock by light. Cell 84:677–685.

Konopka RJ, Benzer S (1971) Clock mutants of *Drosophila melanogaster*. Proc Natl Acad Sci USA 68:2112–2116.

Konopka RJ, Hamblen-Coyle MJ, Jamison CF, Hall JC (1994) An ultrashort clock mutation at the *period* locus of *Drosophila melanogaster* that reveals some new features of the fly's circadian system. J Neurogenet 9:189–216.

Laemmli UK (1970) Cleavage of structural proteins during the assembly of the head of bacteriophage T4. Nature 227:680–685.

Laski FA, Rio DC, Rubin GM (1986) Tissue specificity of *Drosophila* P element transposition is regulated at the level of mRNA splicing. Cell 44:7–19.

Lee C, Parikh V, Itsukaichi T, Bae K, Edery I (1996) Resetting the *Drosophila* clock by photic regulation of PER and a PER-TIM complex. Science 271:1740–1744.

Lindsley DL, Zimm GG (1992) The genome of *Drosophila melanogaster*. San Diego: Academic.

Liu X, Lorenz L, Yu Q, Hall JC, Rosbash M (1988) Spatial and temporal expression of the period gene in *Drosophila melanogaster*. Genes Dev 2:228–238.

Liu X, Yu Q, Huang ZJ, Zwiebel LJ, Hall JC, Rosbash M (1991) The strength and periodicity of D. melanogaster circadian rhythms are differentially affected by alterations in *period* gene expression. Neuron 6:753–766.

Liu X, Zwiebel LJ, Hinton D, Benzer S, Hall JC, Rosbash M (1992) The *period* gene encodes a predominantly nuclear protein in adult *Drosophila*. J Neurosci 12:2735–2744.

Monsma S, Ard R, Lis J, Wolfner MF (1988) Localized heat-shock induction in *Drosophila melanogaster*. J Exp Zool 247:279–284.

Myers MP, Wager-Smith K, Rothenfluh-Hilfiker A, Young MW (1996) Light-induced degradation of TIMELESS and entrainment of the *Drosophila* circadian clock. Science 271:1736–1740.

Rechsteiner M, Rogers S, Rote K (1987) Protein structure and intracellular stability. Trends Biochem Sci 12:390–394.

Robertson HM, Preston CR, Phillis RW, Johnson-Schlitz DM, Benz WK, Engels WR (1988) A stable genomic source of P element transposase in *Drosophila melanogaster*. Genetics 118:461–470.

Rogers S, Wells R, Rechsteiner M (1986) Amino acid sequences common to rapidly degraded proteins: the PEST hypothesis. Science 234:364–368.

Rosbash M (1995) Molecular control of circadian rhythms. Curr Opin Genet Dev 5:662–668.

Rubin GM, Spradling AC (1982) Genetic transformation of *Drosophila* with transposable element vectors. Science 218:348–353.

Rutila JE, Edery I, Hall JC, Rosbash M (1992) The analysis of short-period circadian rhythm mutants suggests features of *D. melanogaster period* gene function. J Neurogenet 8:101–113.

Rutila JE, Zeng H, Le M, Curtin KD, Hall JC, Rosbash M (1996) The $tim^{SL}$ mutant of the Drosophila rhythm gene *timeless* manifests allele-specific interaction with *period* gene mutants. Neuron 17:921–929.

Sehgal A, Price JL, Man B, Young MW (1994) Loss of circadian behavioral rhythms and *per* RNA oscillations in the *Drosophila* mutant *timeless*. Science 263:1603–1606.

Sehgal A, Rothenfluh-Hilfiker A, Hunter-Ensor M, Chen Y, Myers MP, Young MW (1995) Rhythmic Expression of *timeless*: a basis for promoting circadian cycles in *period* gene autoregulation. Science 270:808–810.

Siwicki KK, Eastman C, Peterson G, Rosbash M, Hall JC (1988) Antibodies to the *period* gene product of Drosophila reveal diverse tissue distribution and rhythmic changes in the visual system. Neuron 1:141–150.

Smith RF, Konopka RJ (1982) Effects of dosage alterations at the *per* locus on the period of the circadian clock of *Drosophila*. Mol Gen Genet 183:30–36.

Sokolove PG, Bushell WN (1978) The chi square periodogram: its utility for analysis of circadian rhythms. J Theor Biol 72:131–160.

Thummel CS, Boulet AM, Lipshitz HD (1988) Vectors for P-element-mediated transformation and tissue culture transfection. Gene 74:445–456.

van Gelder R, Krasnow MA (1996) Circadian rhythms: partners in time. Curr Biol 6:244–246.

Vosshall LB, Young MW (1995) Circadian rhythms in *Drosophila* can be driven by *period* expression in a restricted group of central brain cells. Neuron 15:345–360.

Vosshall LB, Price JL, Sehgal A, Saez L, Young MW (1994) Specific block in nuclear localization of period protein by a second clock mutation, *timeless*. Science 263:1606–1609.

Wheeler DA, Hamblen-Coyle MJ, Dushay MS, Hall JC (1993) Behavior in light-dark cycles of *Drosophila* mutants that are arrhythmic, blind, or both. J Neurogenet 8:67–94.

Wood KV (1995) Marker proteins for gene expression. Curr Opin Biotech 6:50–58.

Yu Q, Jacquier AC, Citri Y, Colot HV, Hall JC, Rosbash M (1987) Molecular mapping of point mutations in the *period* gene that stop or speed up biological clocks in *Drosophila melanogaster*. Proc Natl Acad Sci USA 84:784–788.

Zeng H, Hardin PE, Rosbash M (1994) Constitutive overexpression of the *Drosophila period* protein inhibits *period* mRNA cycling. EMBO J 13:3590–3598.

Zeng H, Quian Z, Myers MP, Rosbash M (1996) A light entrainment mechanism for the *Drosophila* circadian clock. Nature 380:129–135.

Zerr DM, Hall JC, Rosbash M, Siwicki KK (1990) Circadian fluctuations of *period* protein immunoreactivity in the CNS and the visual system of *Drosophila*. J Neurosci 10:2749–2762.

Zwiebel LJ, Hardin PE, Liu X, Hall JC, Rosbash M (1991) A post-transcriptional mechanism contributes to circadian cycling of a per-$\beta$-galactosidase fusion protein. Proc Natl Acad Sci USA 88: 3882–3886.